Chemokines cooperate with TNF to provide protective anti-viral immunity and to enhance inflammation

Alí Alejo[1,*], M. Begoña Ruiz-Argüello[1,*], Sergio M. Pontejo[2], María del Mar Fernández de Marco[2], Margarida Saraiva[3], Bruno Hernáez[2] and Antonio Alcamí[2, 3, †]

[1]Centro de Investigación en Sanidad Animal; Instituto Nacional de Investigación y Tecnología Agraria y Alimentaria, Valdeolmos, Madrid, 28130, Spain.

[2]Centro de Biología Molecular Severo Ochoa (Consejo Superior de Investigaciones Científicas and Universidad Autónoma de Madrid), Cantoblanco, Madrid, 28049, Spain.
[3]Department of Medicine, University of Cambridge, Addenbrooke's Hospital, Cambridge, CB2 2QQ, United Kingdom.

Present address M. B. R.-A., Progenika Biopharma, Derio, Spain; S. M. P., National Institutes of Health, Bethesda, Maryland 20892, USA: M. S., Institute for Molecular and Cell Biology, 4200-135 Porto, Portugal; M. F. M., Animal & Plant Health Agency, Addlestone, Surrey KT15 3NB, UK.

* A. Alejo and M.B.R.-A. contributed equally to this work

CONDENSED TITLE: Poxviral CrmD is an essential virulence factor

[†]AUTHOR FOR CORRESPONDENCE:

Antonio Alcamí, aalcami@cbm.csic.es Phone: +34 911964560, Fax: +34 911964420

21 **ABSTRACT**

22 The role of cytokines and chemokines in anti-viral defense has been demonstrated, but
23 their relative contribution to protective anti-viral responses *in vivo* is not fully
24 understood. Cytokine response modifier D (CrmD) is a secreted receptor for TNF and
25 lymphotoxin containing the smallpox virus-encoded chemokine receptor (SECRET)
26 domain and is expressed by ectromelia virus, the causative agent of the smallpox-like
27 disease mousepox. Here we show that CrmD is an essential virulence factor that
28 controls natural killer cell activation and allows progression of fatal mousepox, and
29 demonstrates that both SECRET and TNF binding domains are required for full CrmD
30 activity. Vaccination with recombinant CrmD protects animals from lethal mousepox.
31 These results indicate that a specific set of chemokines enhance the inflammatory and
32 protective anti-viral responses mediated by TNF and lymphotoxin, and illustrate how
33 viruses optimize anti-TNF strategies with addition of a chemokine binding domain as
34 soluble decoy receptors.

INTRODUCTION

A unique immune evasion mechanism employed by poxviruses and herpesviruses is the production of soluble binding proteins or secreted versions of host receptors that neutralize cytokines[1-4]. The poxvirus homologues of host tumour necrosis factor TNF (TNF) receptors (vTNFRs) block the pro-inflammatory activity of some TNF superfamily (TNFSF) ligands. Five vTNFRs have been described in poxviruses, a viral homologue of host TNFSF receptor CD30 and four TNF inhibitors named cytokine response modifier B (CrmB), CrmC, CrmD and CrmE. vTNFRs are differently expressed among viral species and show distinct binding and inhibitory properties[5-13]. While CrmE and CrmC are specific TNF inhibitors, CrmD and CrmB block TNF and lymphotoxin α (LTα). Furthermore, we have recently described that vTNFRs can inhibit membrane TNF and that CrmD and CrmB neutralize another TNFSF ligand, LTβ[14,15]. In addition to the cysteine-rich domains (CRDs), characteristic of the ligand binding region of cellular TNFRs, CrmB and CrmD have a C-terminal domain unrelated to host proteins that binds chemokines and was named SECRET (for smallpox virus-encoded chemokine receptor) domain[16]. The crystal structure of the CrmD SECRET domain showed a beta-sandwich fold similar to that of the viral chemokine binding proteins (vCKBPs) 35-kDa and A41, but a different chemokine interaction region may confer its distinct narrower binding specificity[17-19]. Such variety of activities may provide poxviruses the ability to differentially block chemokines involved in distinct anti-viral responses, to inhibit chemokines at different stages of infection in the host or to simultaneously inhibit chemokines and TNF. Interestingly, the beta-sandwich fold of vCKBPs has also been observed in other unrelated poxviral proteins including CPXV203, a major histocompatibility complex I binding protein encoded by cowpox

virus (CPXV), and GIF, the granulocyte-macrophage colony-stimulating factor and interleukin 2 inhibitor of the parapox Orf virus [4,20]. To reflect such diverse range of immunomodulatory activities this folding has been named as poxvirus immune evasion domain[4,20].

ECTV is a mouse-specific orthopoxvirus[21,22] genetically related to vaccinia virus (VACV), variola virus (VARV) (the causative agent of human smallpox) and monkeypox virus (MPXV)[23,24], a human pathogen whose incidence is increasing due to the cessation of mass smallpox vaccination in Africa[25,26]. Susceptible strains of mice infected with ECTV develop mousepox, a severe disease that constitutes a good model for smallpox. ECTV infection of susceptible mouse strains via the s.c. route has been exploited as a model of generalized virus infections, genetic resistance to disease, and viral immunology[21,22,27]. In ECTV, CrmD is the only secreted TNFR. Similarly, both VARV and MPXV express a single vTNFR with similar characteristics, CrmB. By contrast, CPXV expresses four distinct vTNFRs[13]. In addition, ECTV and other poxviruses encode intracellular proteins that inhibit TNF-induced signalling, underscoring the importance of TNF in antiviral reponses[18,28].

However, our knowledge of the role of TNF and LT in the control of poxviral infections *in vivo* is limited. Knockout mice lacking both TNFR1 and TNFR2 showed a slightly increased susceptibility to ECTV and elevated viral replication, with 60% of the infected animals succumbing to mousepox while all WT mice resisted infection [29]. A direct antiviral activity of TNF has been proposed using a recombinant VACV expressing TNF[30]. This direct effect was substantiated in TNF-deficient mice infected with VACV, which showed a modest (two-fold) reduction in LD50 as compared to WT mice, that was accompanied by an increased virus load but not by a diminished T cell response[31]. Although resistance to mousepox was associated with Th1-like cytokine

85 expression, including TNF, blockade of TNF using monoclonal antibodies did not affect
86 the generation of NK cell and CTL responses, virus clearance or resistance to ECTV
87 infection[32] and treatment with TNF did only reduce the mortality rate from 100% to
88 70% in susceptible BALB/c mice[33]. VACV-infected TNFR2-deficient C57BL6 mice
89 produced higher viral titers in spleens and livers and reduced numbers of inflammatory
90 cell foci in the liver, as compared to WT mice[34].

91 A contribution of vTNFRs to pathogenesis was initially shown with a CPXV lacking
92 CrmB, but expressing other vTNFRs, which displayed an increased LD50 in infected
93 mice after intracranial inoculation, a route of infection not natural for poxviruses[35].
94 Inactivation of a CrmB homologue (M-T2) from myxoma virus reduced clinical signs
95 of illnesss in infeced rabbits[36]. However, the reported attenuation in the initial studies
96 cannot be formally atributed solely to the absence of the vTNFR since the selection of
97 inadvertent mutations elsewhere in the viral genome was not controlled with the
98 construction of revertant viruses or by sequencing the complete viral genome.
99 Additional studies with the VACV vaccine strain USSR showed that deletion of CrmC
100 or CrmE caused no effect in virulence or a very mild attenuation not affecting mortality,
101 respectively, after i.n. infection of mice[37]. Recombinant VACV strain Western Reserve
102 expressing CrmC, CrmB or CrmE displayed increased virulence less than 10-fold in an
103 i.n. mouse model, but high virus doses were required to cause disease because the
104 recombinant viruses were deficient in the thymidine kinase gene[37,38]. Definitive studies
105 addressing the role of vTNFRs in viral pathogenesis using virulent poxviruses in their
106 natural host are lacking.

107 Here we show that CrmD is an essential virulence factor as deletion of CrmD from
108 ECTV resulted in a dramatic attenuation phenotype, generating an avirulent virus that
109 induced strong NK cell and CD8 T cell responses but did not establish fatal mousepox.

This demonstrates a critical role of TNF and a reduced set of chemokines in anti-viral defense. Moreover, this unique model of virus infection in a natural host, together with the construction of mutant viruses, allowed us to dissect the relative contribution of TNF and chemokine activities *in vivo*. We report that expression of the anti-TNF (CRD domain) or anti-chemokine (SECRET domain) activities of CrmD are not sufficient on their own to confer full virulence to ECTV, suggesting that the function of some chemokines complement TNF in protection against viruses. Furthermore, immunization of mice with recombinant CrmD protected from a lethal ECTV challenge.

RESULTS

ECTV CrmD is an essential virulence factor

To address the role of CrmD in mousepox pathogenesis, we generated recombinant ECTVs in the Naval strain (Fig. 1a). An ECTV CrmD deletion mutant was obtained (ECTVΔCrmD) with both copies of the *CrmD* gene deleted. As a control for the selection of inadvertent mutations in other genes during the generation of ECTVΔCrmD, a revertant virus (ECTVRevCrmD) with both copies of the full length *CrmD* gene restored was constructed. To study the differential contribution of TNF- *vs* chemokine- inhibitory activities of CrmD, a virus expressing only the TNF binding domain of CrmD, composed of CRDs (ECTVRevCRD), was constructed. The complete genome sequence of ECTVRevCRD confirmed the correct incorporation of two copies of the truncated CrmD TNF binding domain and the absence of additional mutations. Replication of recombinant viruses was comparable to that of the parental ECTV (Fig. 1d). As expected, ECTVΔCrmD-infected cell supernatants showed neither expression of CrmD protein nor TNF blocking activity, whereas infections with either parental or revertant viruses showed similar levels of CrmD and TNF inhibitory activity (Fig. 1b, c). ECTVRevCRD-infected cells expressed a truncated CrmD protein that inhibited TNF activity as efficiently as supernatants from ECTV- or ECTVRevCrmD-infected cells. As a control, all samples expressed similar amounts of the secreted 35-kDa vCKBP[39] (Fig. 1b).

Viral virulence was determined in susceptible BALB/c mice s.c. in the footpad (Table 1). Only four out of 20 animals infected with 10 PFU of either parental or ECTVRevCrmD viruses survived the disease, with an estimated LD50 of less than 10

PFU. In contrast, ECTVΔCrmD was severely attenuated, as only one animal out of five died when 10^7 PFU were administered while all other mice survived. This difference of at least six orders of magnitude in LD50 of ECTVΔCrmD as compared to ECTV indicated that CrmD is an essential virulence factor in mousepox and that its deletion renders ECTV practically avirulent. Reintroduction of both copies of the full length CrmD into the genome of ECTVΔCrmD restored virulence, demonstrating an exclusive CrmD-mediated effect. Interestingly, the LD50 estimated for mice infected with ECTVRevCRD was around 10^5 PFU, showing attenuation of the virus lacking only the chemokine inhibitory domain as compared to parental and revertant ECTVRevCrmD viruses. This indicated that the SECRET domain was essential for pathogenesis.

ECTV CrmD controls an inflammatory reaction *in vivo*

Infected animals were monitored daily for weight loss, signs of illness and footpad swelling (Fig. 2). As shown for two viral doses (10 PFU and 1,000 PFU per animal), mice infected with ECTVΔCrmD suffered less severe weight loss and signs of illness as compared to mice infected with parental or revertant ECTVRevCrmD viruses. Weight of ECTVΔCrmD-infected mice did not drop below 95% of their initial value and mean scores peaked at around 1 in a scale ranging from 0 for a healthy individual to 4 for a severely diseased animal. ECTVΔCrmD-infected mice had fully recovered from disease by 16 d post-infection (dpi). Similarly, ECTVRevCRD-infected mice showed reduced weight loss and signs of illness, with surviving mice fully recovering (Fig. 2). In this case, the differences were more apparent at the lower doses. The thickness of the site of virus inoculation (footpad) was assessed as a measure of inflammatory response. In ECTV and ECTVRevCrmD-infected animals only a few individuals responded with

166 footpad swelling, starting at 10 dpi, when most of the mice had succumbed to infection.
167 However, ECTVΔCrmD-infected mice showed a strong footpad swelling starting 2-3
168 days earlier and peaking by 10-11 dpi at values higher than those observed with parental
169 virus (Fig. 2). Thus, CrmD efficiently controls footpad swelling, consistent with its
170 proposed immunomodulatory role (Fig. 3a, b).

171 In mice infected with ECTVRevCRD, expressing the TNF but not the chemokine
172 blocking activity of CrmD, footpad swelling was significantly delayed as compared to
173 that observed in the absence of CrmD, showing that TNF activity *in vivo* is crucial for
174 an inflammatory reaction. However, inflammation did still occur, which could reflect an
175 incomplete blockade of TNF activity as well as the activity of other proinflammatory
176 stimuli, such as the chemokines not blocked due to the absence of the SECRET domain
177 in this virus. Haematoxilin and eosin (H&E) staining of sections of the footpad of
178 ECTVΔCrmD-infected mice showed the presence of a large inflammatory infiltrate
179 with edema in the dermis, which was not detected or much reduced in ECTV-infected
180 mice (Fig. 3c, d). The infiltrate was composed mainly of lymphocytes (Fig. 3g) and
181 macrophages with a few polymorphonuclear leukocytes. Immunostaining showed the
182 presence of CD4+ T cells (10% CD3+; 12% CD4+) and some B cells (5%), but no
183 CD8+ cells were detected. Sections were stained for expression of Inter Cellular
184 Adhesion Molecule-1 (ICAM-1), an integrin ligand overexpressed on endothelial cells
185 of the postcapillary venules in response to proinflammatory cytokines such as TNF [40].
186 More than 50% of vessels in the footpads of ECTVΔCrmD-infected mice showed
187 intense ICAM-1 staining, while only around 25% of vessels expressed ICAM-1 in
188 ECTV- or ECTVRevCrmD-infected mice (Fig. 3e, f), indicating a role for CrmD in
189 controlling inflammation through TNF inhibition. Our previous studies defined the
190 binding specificity of CrmD for human chemokines[16], and we have characterized here

191 the interaction of CrmD with mouse chemokines (Fig. 4). Consistent with the anti-
192 chemokine activity of CrmD, immunohistochemistry of footpad sections showed that
193 approximately 30% of the infiltrating cells in ECTVΔCrmD-infected mice by 7 dpi
194 expressed the CCR10 chemokine receptor (Fig. 3h) whereas no CCR10-expressing cells
195 were observed in ECTV infections. The CrmD SECRET domain interacts with the
196 mouse chemokines Ccl28 and Ccl27, the latter with higher affinity (Fig. 4), which are
197 recognized by CCR10. This indicates that the SECRET domain may contribute to the
198 inhibition of chemokine-directed cell migration *in vivo*. Consistently, a similar amount
199 of CCR10-expressing cells was detected in the footpad infiltrate of ECTVRevCRD-
200 infected mice.

201

202

203 **Virus replication is restricted in the absence of ECTV CrmD**

204 The extent of viral replication and dissemination in the host in the absence of CrmD was
205 analysed. Viral replication was apparently not hindered at the site of inoculation, as
206 assessed by anti-virus and anti-CrmD staining of sections from footpads of infected
207 mice at 7 dpi (Fig. 5c-h). This also showed that ECTV replicates *in vivo* in the absence
208 of CrmD and the stability of the truncated CRD protein *in vivo*. Staining of sections
209 from footpads of uninfected mice showed the specificity of the anti-virus and anti-
210 CrmD antibodies (Supplementary Fig. 1). As shown in Fig. 5a and b, by 3 dpi, all four
211 viruses had reached both the spleen and liver, with no significant differences in the viral
212 titers among them, suggesting that the absence of CrmD did not affect the capacity of
213 the virus to spread to its secondary replication sites. However, both the parental and the
214 revertant ECTVRevCrmD viruses reached high titers by 7 dpi in the spleen (Fig. 5a)

and liver (Fig. 5b), whereas ECTVΔCrmD titers were reduced by 2 and 4 log units in these organs, respectively. This shows that ECTV replication in spleen and liver is controlled by the host in the absence of CrmD. The expression of the TNF inhibitory domain of CrmD by ECTVRevCRD fully restored ECTV infectivity in spleen, but not in the liver, suggesting that the relative contribution of TNF activity for protection against virus replication *in vivo* might be organ-dependent. These results also suggest that chemokine inhibition by the SECRET domain may be especially important for virus replication in the liver. All mice infected with either ECTVΔCrmD or ECTVRevCRD survived the infection and virus was being cleared by 11 dpi (Fig. 5a, b). Limited virus replication in the absence of CrmD was accompanied by reduced necrosis of the infected organs (Fig. 5j, m, Table 2, Supplementary Fig. 2), which was also apparent in the liver in the case of ECTVRevCRD-infected mice (Fig. 5n and Table 2). Additionally, an increased inflammation of the liver at 7 or 11 dpi was observed in the absence of CrmD (Fig. 5m and Table 2). Altogether, these results showed that in the absence of CrmD ECTV replication can be controlled by the host and suggest that reduced liver damage is the cause for survival of infected mice.

ECTV requires inhibition of chemokines and TNF for virulence

To further assess the role of the CrmD SECRET domain in mousepox pathogenesis, a recombinant virus was constructed in which CrmD was replaced by a CrmD variant bearing a point mutation (N77F) that lacks TNF binding and inhibitory activity while maintaining its chemokine inhibitory activity. Fig. 6 shows the binding and biological properties of the purified recombinant CrmD N77F mutant, demonstrating that it has lost the TNF inhibitory activity but retains the ability to inhibit chemokine-mediated

240 cell migration, with a similar potency as that shown by CrmD. The complete genome
241 sequence of this virus, termed ECTVRevSECRET, confirmed the incorporation of two
242 copies of the CrmD N77F mutant gene and that no other mutations that may influence
243 virus virulence were present. ECTVRevSECRET replicated efficently in cell culture
244 and expressrd the mutated protein to similar levels than the parental virus, considering
245 the loading control of vCKBP (Fig. 7b). As expected, supernatants of
246 ECTVRevSECRET-infected cells did not show TNF inhibitory activity (Fig. 7c).

247 The virulence of ECTVRevSECRET was assessed in susceptible BALB/c mice infected
248 s.c. in the footpad with virus doses ranging from 10^4 to 10^6 PFU per animal. With only
249 one animal out of 5 succumbing to mousepox after infection with the highest dose
250 tested (Fig. 7d, e), ECTVRevSECRET was nearly as severely attenuated as the
251 ECTVΔCrmD mutant. ECTVRevCRD, expressing the TNF binding domain, was
252 slightly more virulent than ECTVRevSECRET, expressing the chemokine binding
253 activity. ECTVRevSECRET was able to replicate *in vivo* and to reach the spleen, but
254 replicated to levels lower than ECTVRevCRD and ECTVRevCrmD (Fig. 7f). As shown
255 before, infection with 10^6 PFU of ECTVΔCrmD produced a strong footpad swelling
256 starting at 5 dpi, that was impaired by expression of CrmD (ECTVRevCrmD) or the
257 TNF binding domain of CrmD (ECTVRevCRD) (Fig. 7e). Expression of the chemokine
258 binding activity of CrmD by ECTVRevSECRET was also able to block this
259 inflammatory reaction, albeit to a reduced degree (Fig. 7e). Altogether, these results
260 showed that the SECRET domain chemokine inhibitory activity per se is not able to act
261 as a virulence factor, suggesting that its role in pathogenesis is only apparent when the
262 TNF inhibitory activity is also expressed by the virus.

263

264 **Modulation of NK cell and CD8 T cell responses by CrmD**

265 It has been shown that upon footpad inoculation of ECTV, the NK cell response during
266 the first 4 dpi in the draining popliteal LN (DPLN) and the T cell response at late stages
267 (peak at 7 dpi) in the secondary organs are required to survive lethal mousepox [21,22]. To
268 understand the mechanisms by which ECTV CrmD allows viral replication and whether
269 it impairs the immune response, we studied the early NK cell response and the late T
270 cell response against the different recombinant viruses in the DPLN at 2 dpi and in the
271 spleen at 7 dpi, respectively.

272 The NK cell population (CD3-DX5+) of all the infected groups represented around 3%
273 of the cells in the DPLN whereas it was less than 1% in the PBS-inoculated group (Fig.
274 8a, c). Furhermore, no differences in the total number of NK cells present in the DPLN
275 at 2 dpi were found among the different infected groups (Fig. 8b). This suggested that
276 CrmD is not involved in controling the recruitment of NK cells to early virus replication
277 sites. However, differences in the activation status of NK cell populations were found.
278 In the PBS-inoculated group less than 2% of NK cells were activated, as assessed by
279 granzyme B expression (Fig. 8d). Conversely, in mice infected with recombinant
280 viruses lacking the TNF blocking ability, ECTVΔCrmD and ECTVRevSECRET, more
281 than 20% of NK cells were activated. In contrast, viruses expressing the TNF binding
282 domain, ECTVRevCRD and ECTVRevCrmD, significantly controlled NK cell
283 activation, reducing by half the % of granzyme B+ NK cells (Fig. 8d). These results
284 suggested that the anti-TNF activity of CrmD impairs the early NK cell activation in
285 response to ECTV infection.

286 At 7 dpi, infection with the CrmD-expressing virus produced an almost complete
287 elimination of CD8 T cells from the spleens (Fig. 8a, e). It is important to clarify that

288 although the representative dot blot in Fig. 8a (bottom panel) still shows a 1.9% of CD8
289 T cells in the spleen of ECTVRevCrmD-infected mice, this was only slightly above the
290 staining observed with the corresponding isotype control (1.3%). In addition, only 40%
291 of the analyzed cells fell inside the lymphocyte gate in this group, whereas the analysis
292 gate gathered more than 80% of the cells in all the other groups (Supplementary Fig. 3).
293 These two factors explain the almost complete depletion of CD8 cells in mice infected
294 with ECTVRevCrmD shown in Fig. 8e. This splenic lymphopenia has been observed
295 previously in ECTV lethal infections[41-43]. In mice infected with either ECTVΔCrmD,
296 ECTVRevCRD or ECTVRevSECRET, however, CD8 T cells were detectable and
297 efficiently activated in response to infection (Fig. 8a, e and f). This showed that the
298 presence of both the TNF and chemokine binding domains in the CrmD protein is
299 necessary for the inhibition and elimination of CD8 T cells in the spleen, and for full
300 virulence of ECTV.

301

302

303 **Immunization with ECTV CrmD protects from fatal mousepox**

304 As ECTV infection was severely attenuated in the absence of ECTV CrmD, we
305 hypothesized that a blockade of ECTV CrmD protein may prevent the development of
306 mousepox. To test this, we immunized susceptible mice with purified recombinant
307 ECTV CrmD protein and challenged them with a lethal dose (100-fold LD50) of ECTV,
308 to test the induction of an efficient protective response. Sera from CrmD-immunized
309 mice (14 out of 15 mice), but not from control mice, neutralized the ability of CrmD to
310 inhibit TNF activity in a cytotoxicity assay (Fig. 9a, 2 µl dose) causing <50% cell
311 viability. Addition of a lower amount of sera in the TNF biological assay identified a

312 weaker CrmD neutralization activity in 3 of the 5 mice that succumbed to infection after
313 CrmD immunization (Fig. 9a, 1 µl dose). After ECTV inoculation, mice previously
314 immunized with CrmD developed mousepox signs and suffered weigth loss to a similar
315 degree as those injected with PBS (Fig. 9b, c). However, the immunized mice showed
316 very early and acute footpad swelling in response to infection (Fig. 9d), reminiscent of
317 that observed in ECTVΔCrmD-infected mice and suggesting that ECTV CrmD activity
318 produced by WT ECTV was neutralized in these animals. Moreover, 67% of the CrmD
319 immunized mice survived infection and had fully recovered by 30 dpi, while all the PBS
320 injected mice had died by 10 dpi (Fig. 9e).

321

322

323 **DISCUSSION**

324 The results presented here show that ECTV CrmD is an essential factor for mousepox
325 virulence and that both its TNF and chemokine inhibitory activities contribute to its
326 immunomodulatory role. ECTV replication in secondary replication organs, spleen and
327 liver, was impaired in the absence of CrmD. The most probable cause of death during
328 mousepox is liver failure due to extensive viral replication[32]. Therefore, reduced viral
329 replication and hence necrosis in this organ may account for survival of mice infected
330 with ECTV lacking either the full length CrmD, or the anti-TNF or anti-chemokine
331 activities of the protein. Additionally, expression of CrmD in the spleen and liver will
332 block anti-viral responses in these organs, consistent with an increased inflammatory
333 response in the liver of ECTVΔCrmD- and ECTVRevCRD-infected mice.

334 Deletion of the *CrmD* gene from ECTV results in one of the most profound effects on
335 virulence described in poxviruses[17,18]. Previous reports have shown that inactivation of

other vTNFRs secreted by VACV, CPXV and myxoma virus causes limited viral attenuation, and some reports are not conclusive[35-37]. Similarly, inactivation of vCKBPs, 35-kDa and A41 proteins, from poxvirus genomes causes increased leukocyte recruitment to sites of infection without major effects on disease progression or mortality, or a slight attenuation as a result of reduced inflammatory pathology[17,18]. Interesting, deletion of the ECTV type I IFN binding protein, which targets a different cytokine, rendered the virus avirulent to a degree similar to that we observed after CrmD deletion[44] . This suggests a possible link between the type I IFN and the TNF/LT/chemokine anti-viral host responses, as the link described for the type I IFN and nuclear factor kappa B pathways[45]. Increased LT signalling in the absence of CrmD could contribute to the induction of the IFN response, as described for murine cytomegalovirus[46], restricting virus replication through increased type I IFN signalling to immune cells or direct effects on infected cells. In accordance with this, TNF and IFN may act synergistically in anti-viral defense[47]. Also, a role of the LT network in controlling the type I IFN response has been proposed[48].

Previous data suggested a role for TNF-induced signalling in mousepox pathogenesis, as transgenic resistant mice lacking functional TNFR1 and TNFR2 became susceptible to ECTV[29]. Consistently, treatment of susceptible BALB/c mice with murine TNF hindered ECTV replication and mortality to some extent[33]. However, TNF had a relatively minor role during ECTV or related poxvirus infections in terms of impact on LD50. Strikingly, the lack of the secreted TNF binding protein CrmD has a profound effect, reducing virulence almost completely. While specific experimental setups may account for these differences, they indicate a role of CrmD beyond inhibition of soluble TNF, which may include inhibition of LTα, LTβ or chemokines. In addition, we have recently demonstrated that CrmD and other vTNFRs interact with membrane TNF and

inhibit its cytotoxic activity[14]. Further, CrmD may trigger reverse signaling in membrane TNF-bearing cells, as shown for viral CD30[7], and this may influence the anti-viral response.

This CrmD-membrane TNF interaction might also explain the impaired activation of NK cells in the DPLN of mice infected with ECTVRevCrmD and ECTVRevCRD. NK cells are required at early stages to curb ECTV dissemination from the lymph nodes to the spleen and liver and ultimatelly, to survive to fatal mousepox[41,49]. Despite historically considered effector cells of the innate immunity, NK cell responses are greatly modulated by dendritic cells (DC)[50,51], being more efficient when both cells are in direct contact [50,51], and this is important for defense against other viral infection[52]. Accordingly, DC-depleted C57BL/6 mice are susceptible to ECTV[53]. The DC-NK crosstalk is mediated in mouse and human by the engagement of DC membrane TNF, but not soluble TNF, with NK TNFR2[54,55]. Therefore, CrmD or the truncated TNF binding domain may be blocking the membrane TNF-TNFR2 interaction hindering an efficient DC-NK cell crosstalk. A weak NK cell activity might explain the high viral titers of ECTV and ECTVRevCRD detected later in the spleen, whereas the dissemination of ECTVRevSECRET and the CrmD deletion mutant is curbed by a potent early NK cell response. After 4 dpi NK cells are no longer required for resistance to ECTV challenge and the T cell response takes over[41]. At day 7 in the spleen, we observed a depletion of CD8 lymphocytes in mice infected with ECTV expressing CrmD, however, an efficient CD8 response was mounted against all the other viruses tested here. Of note, this CD8 cell depletion did not correlate with viral loads in the spleen since ECTVRevCRD, which reaches equally high viral titers, did not cause lymphopenia. This result suggests that both CrmD immunomodulatory activities, anti-TNF and anti-chemokines, are required for complete control of the T cell response in

386 the spleen. Consistently, the SECRET domain binds Cxcl11, one of the ligands of the
387 chemokine receptor CXCR3 that enhances the ability of CD8 T cells to locate VACV-
388 infected cells and to exert anti-viral effector functions[56]. In agreement with a role of
389 both TNF and chemokines in T cell responses, neutralization with anti-TNF antibodies
390 does not affect the splenic late CTL response against ECTV in C57BL/6 mice[32].
391 However, this might be an indirect effect since splenic lymphopenia has also been
392 observed in other ECTV lethal infections where the host ability to mount an efficient
393 TNF and chemokine response is intact[41,42].

394 Here we show that ECTV CrmD efficiently inhibits the establishment of a
395 proinflammatory state at the site of virus inoculation, as evidenced by the increased
396 ICAM-1 expression observed in its absence. The ability of CrmD to block TNF and LT
397 activity, cytokines that induce the expression of ICAM-1 on endothelial cells, could
398 account for this[15,16]. In the absence of CrmD, an increased inflammatory infiltrate was
399 observed both in the footpad and in the liver, consistent with the chemokine inhibitory
400 function of its SECRET domain. More specifically, an important fraction of the footpad
401 infiltrate was composed of cells bearing the chemokine receptor CCR10, which
402 supports migration of lymphocytes towards Ccl28 and Ccl27. Both chemokines are
403 bound with high affinity by CrmD and expressed by skin keratinocytes in response to
404 TNF and other proinflammatory stimuli[16,57]. Indeed, Ccl27 is important in T-cell
405 mediated skin inflammation *in vivo*[58]. Thus, the potent anti-inflammatory activity of
406 CrmD may be due to its ability to inhibit either TNF/LT as well as a set of chemokines.
407 Consistent with this, VARV CrmB, with properties similar to CrmD, blocks cell
408 migration induced after epicutaneous application of murine TNF[59].

409 The infection of mice with ECTVRevCRD or ECTVRevSECRET expressing the anti-
410 TNF/LT or anti-chemokine activity of CrmD, respectively, allowed us to address the

411 contribution of TNF/LT *vs.* chemokines to inflammatory and protective responses *in*
412 *vivo*. Interestingly, ECTVRevCRD was not able to efficiently control the inflammatory
413 infiltrate observed in ECTVΔCrmD-infected mice, in spite of the well-documented and
414 potent pro-inflammatory function of TNF. This suggested that the activity of the mouse
415 chemokines targeted by the SECRET domain (Ccl24, Ccl25, Ccl27, Cxcl11, Cxcl12β,
416 Cxcl13 and Cxcl14) was sufficient to control cell migration and to trigger inflammation
417 when TNF was neutralized by the truncated CrmD protein. The delay in the appearance
418 of the inflammatory infiltrate in ECTVRevCRD-infected mice as compared to that
419 observed with ECTVΔCrmD, probably reflects TNF blockade at the inoculation site
420 and suggests the involvement of TNF in triggering the initial response *in vivo*. It is
421 important to note that the infiltrating cells are probably contributing to an increased
422 expression of cytokines, and thus chemokine blockade by the CrmD SECRET domain
423 expressed in ECTVRevSECRET infections may impair localized TNF expression.
424 Limited recruitment of cytokine producing cells into the sites of infection may be a
425 general principle in host-pathogen interactions and help pathogens escape the host
426 response, as shown in a *Leishmamia major* mouse model of dermal infection[60] and in
427 *Listeria monocytogenes*-infected mice, where Ccl2-induced recruitment of TNF and
428 iNOS producing cells to the spleen mediates an effective innate immune response[61].

429 The reasons for the dramatic attenuation phenotype of the CrmD mutant could be
430 related to the nature of the chemokines targeted and/or the inhibitory mechanism. The
431 CrmD SECRET domain is different from the 35-kDa vCKBP in the specific set of
432 chemokines blocked[17,18]. The VACV A41 protein and its ECTV Naval orthologue E163
433 bind a number of chemokines including those recognized by the SECRET domain, but
434 they do not block chemokine interaction with its receptor and is rather proposed to
435 dissipate chemokine chemotactic gradients *in vivo* by targeting the glycosaminoglycan

binding site of chemokines[17,18]. Thus the 35-kDa vCKBP and A41 ECTV orthologues are probably involved in controlling different aspects of the anti-viral host response. Moreover, ECTV encodes two SECRET domain-containing proteins, named E12 and E184, that show the same chemokine binding specificity[16] but these proteins are not able to compensate for the loss of the CrmD SECRET domain. The phenotype of ECTVrevSECRET, expressing anti-chemokine activity but lacking TNF/LT inhibitory activity, indicates that the SECRET domain needs simultaneous TNF blockade to have a major impact on virus virulence. Additionally, the finding of the SECRET domain on the same molecule than a TNF binding domain might be relevant to ensure an efficient combined effect in the infected host. It is reasonable to propose that the coordinated blockade of cytokines and chemokines by a viral protein could serve as an excellent inhibitor of cell recruitment and the immune response *in vivo*, as shown here for the poxviral CrmD protein and previously for murine cytomegalovirus[62].

The study of the contribution of CrmD to mousepox sheds light into the mechanisms of the pathogenesis of acute viral infections. Importantly, mousepox is a model for human smallpox, a severe human disease caused by VARV and whose pathogenesis has not been extensively studied at the molecular level. VARV and ECTV share secreted immunomodulatory proteins and encode only one vTNFR[13,16]. The VARV protein CrmB has TNF/LT and chemokine inhibitory properties similar to those of ECTV CrmD, but is better adapted to block the human immune system[15,16]. The control of TNF-induced gene expression observed in VARV-infected monkeys suggests that CrmB is expressed during infection[63]. Our results suggest that VARV CrmB is an important virulence factor in smallpox. The same may be true for MPXV, an orthopoxvirus causing a smallpox-like disease in humans with mortality rates of up to 10% that encodes a CrmB orthologue[64]. The fear of either an intentional release of

VARV or the emergence of a poxviral zoonosis, caused by MPXV or other poxviruses[25,26] in a large unvaccinated population have sparked the interest in developing safer vaccines or drugs to prevent or treat human poxviral infections. Although current vaccines have a proven efficacy record, potential risks relating to secondary effects, the increased number of immunocompromised individuals and uncertainty about the duration of protective immunity exist. Thus, alternative strategies for the development of safer vaccines are being currently pursued (reviewed in[65]). Recombinant protein is thought to be safer, and different combinations or single protein vaccination using components from virus particles, which induce neutralizing antibodies, protect from poxvirus infections[66-68]. Our report shows that immunization with recombinant ECTV CrmD protects mice from a lethal mousepox challenge, possibly by an antibody-mediated blockade of CrmD-ligand interaction and clearance of the CrmD protein from the infected host. Similar results have been obtained by vaccinating with the type I IFN binding protein from ECTV[44], and antibodies against this secreted viral protein protect from mousepox [69]. Thus, secreted poxviral immunomodulators can act as effective subunit vaccines in preventing a lethal poxvirus infection in its natural host and could be used singly or in combination with other proteins. It is important to note that the smallpox VACV vaccines Dryvax and Modified VACV Ankara do not express the CrmB protein and will not induce a neutralizing response against CrmB expressed by VARV or MPXV[13]. However, the Dryvax vaccine induced an immune response against viral structural proteins that was sufficient to protect from smallpox.

TNF and chemokines are important in the development of human pathologies unrelated to viral infection. Notably, soluble TNFRs are used to treat a variety of inflammatory conditions in the clinic such as rheumathoid arthritis, ankylosing spondylitis or psoriatic

arthritis[70]. To date soluble versions of the human TNFR2 or monoclonal anti-TNF antibodies are used, although other strategies are under development. The use of vTNFRs in this context has been proposed[9,71], and transgenic mice expressing ECTV CrmD have shown that it can inhibit TNF driven inflammatory reactions *in vivo*[72]. The fact that CrmD acts as a potent anti-inflammatory molecule *in vivo* and that its SECRET domain is important for this activity suggests that addition of a chemokine inhibitory domain to the human soluble TNFRs may increase their clinical efficacy in certain settings. However, this approach should be taken with caution because an antirheumatic drug combining anti-TNF and anti-chemokine activities could be expected to further dampen the already debilitated immune response of patients under anti-TNF therapy, what might worsen the frequent infectious complications observed in these patients[73].

In conclusion, the characterization of the role of CrmD in mousepox pathogenesis has demonstrated a critical role of TNF and a specific set of chemokines in defense from virulent poxvirus infections. The nature of the ligands of CrmD may point to the cytokines and chemokines important in the control of poxviral infections.

METHODS

Cells and viruses

A plaque-purified and fully sequenced ECTV Naval isolate (Naval.Cam) was grown in BSC-1 cells (ATCC CCL-26)[24]. For titration of virus in organs from infected mice, spleen and liver were aseptically removed, weighed and homogeneized and serial dilutions plated on BSC-1 cell monolayers. For infection of mice, virus stocks were semipurified by centrifugation through a 36% sucrose cushion[74]. Viral stocks were routinely tested for the absence of mycoplasma and the endotoxin levels detected usingToxiSensor Chromogenic LAL Endotoxin Assay kit (GenScript) were under 0.3 EU/ml.

Expression and purification of recombinant CrmD proteins

For the generation of anti-CrmD polyclonal rabbit antibodies and immunization experiments, rabbits and mice, respectively, were injected with a recombinant CrmD fused to the Fc portion of a human IgG1 (CrmD-Fc). CrmD-Fc was expressed by recombinant baculoviruses and purified from the supernant of infected Hi5 insect cells (ThermoFisher BTI-TN-5B1-4) by affinity chromatography in a protein A coupled sepharose column. Similarly, a CrmD C-terminally tagged with V5 and 6xHis epitopes was expressed by recombinant baculoviruses as previously described[15]. A N77F mutant of this CrmD-V5-6xHis protein was generated using the QuikChange II Site-Directed mutagenesis kit (Agilent Technologies) and expressed by recombinant baculoviruses[15].

525 **CrmD anti-TNF activity assay**

526 The ability of ECTV CrmD to block TNF-induced cell death was determined as
527 described[16]. Briefly, L929 cells (ATCC CCL-1) were incubated with TNF (R&D
528 Systems, Minneapolis, USA) which had been preincubated or not with recombinant
529 ECTV CrmD protein or supernatants from ECTV-infected cells and cell death
530 determined using the CellTiter OneSolution viability assay (Promega).

531

532 **Chemotaxis assays**

533 The anti-chemokine activity of CrmD wild type and the N77F mutant was assessed by
534 chemotaxis assays using a 96-well ChemoTx plate with a 3-um pore sized filter as
535 previously described[16]. Briefly, MOLT-4 cells (ATCC CRL-1582) were incubated with
536 70 nM of mouse Ccl25 (Peprotech Inc., London, UK) in RPMI 0.1% FBS in the
537 presence or absence of CrmD wild type or N77F at the indicated molar ratios.
538 Unspecific migration in the absence of chemokine was also monitored as reference
539 (media). Cell migration through the filter was allowed to occur during 4 h at 37^{o}C, and
540 subsequently the number of cells that migrated to the bottom well was calculated by
541 interpolation in a standard curve of number of cells using CellTiter Aqueous One
542 Solution assay kit (Promega).

543

544 **Surface Plasmon Resonance**

545 The binding affinity of recombinant CrmD for mouse chemokines (Peprotech Inc.,
546 London, UK) and the ability of wild type CrmD and mutant N77F to interact with

547 mouse TNF (R&D Systems, Minneapolis, USA) and Ccl25 (Peprotech Inc., London,
548 UK) were determined by SPR using a Biacore X biosensor (GE Healthcare).

549 For affinity determinations, recombinant CrmD was immobilized onto a flow cell of a
550 CM4 chip at low density (900 RUs) by the amine coupling protocol. One flow cell was
551 left empty to be used as reference. Increasing concentrations of mouse chemokines were
552 injected in HBS-EP buffer (GE Healthcare) over the chip surface and their binding was
553 recorded for 120 s followed by a 300 s dissociation period. Surface was regenerated
554 with glycin-HCl pH2.0 between injections. Binding sensorgrams were analyzed by the
555 BiaEvaluation software (GE Healthcare) and fitted to a general 1:1 Langmuir binding
556 model.

557 For binding assays, recombinant wild type and N77F CrmD proteins were immobilized
558 on to a flow cell of a CM4 chip at high density (1500 RUs) as explained above. 100 nM
559 of mouse TNF or mouse Ccl25 were injected over the chip in HBS-EP buffer and their
560 association was monitored during 120 s followed by a 120 s dissociation. Binding
561 sensorgrams were processed and analyzed using the BiaEvaluation software.

562

563 **Construction of recombinant ECTVs**

564 Recombinant ECTVs were generated using a transient dominant selection procedure
565 and the selection in the presence of puromycin as previously described[74]. The plasmid
566 pMS30 was constructed for expression of EGFP under a VACV early-late promoter
567 followed by an IRES cassette for expression of the puromycin acetyl transferase gene
568 from the same transcript. For the generation of ECTVΔCrmD, the flanking regions of
569 the *CrmD* gene were PCR-amplified and cloned into the *EcoRI* and *PstI* restriction sites
570 of the polylinker region of pMS30. The 5' flanking region of the *CrmD* gene was

amplified with oligonucleotides CrmD-27 (5'-GCGGAATTCCGATTTAATAACATTCGATTATATAG) and CrmD-11 (5'-CGCGGATCCGGTGTATACGGAACATCTCCAC), and the 3' flanking region of CrmD was amplified with oligonucleotides CrmD18 (5'-CGCGGATCCTAACATGGACGTCGTCGCGTATCATAC) and CrmD28 (5'-GCGCTGCAGCTCTGTAATGATGGACGTTATTTC), to generate the plasmid pMS34 (pΔCrmD). Both flanking regions and the *CrmD* gene were PCR-amplified with oligonucleotides CrmD27 and CrmD28 to generate the plasmid pMS37 (pRevCrmD) that was used for reinsertion of the *CrmD* gene into the ECTVΔCrmD genome and construction of ECTVRevCrmD. The 5´flanking region used for generation of ΔcrmD and the TNF binding domain of CrmD including a stop codon were PCR-amplified using oligonucleotides CrmD27 and CrmD30 (5´-CGCGGATCCTAACAAGAGGTCTTGTTAACAGGATAC) and pMS37 as a template. The resulting PCR product was cloned into the *EcoRI* and *BamHI* sites of pMS34 generating plasmid pAH7. This plasmid was used to generate ECTVRevCRD, which expresses a truncated version of CrmD corresponding to residues M1 to C180. For the generation of ECTVRevSECRET, the CrmD gene contained in pMS37 was mutated by directed single point mutation using the QuickChange II mutagenesis kit (Agilent Technologies) and the primers CrmD43 (AGATGACACCTTTACATCCATTCCTTTTCATAGTCCCGCGTG) and CrmD44 (CACGCGGGACTATGAAAAGGAATGGATGTAAAGGTGTCATCT). These primers introduce a N77F mutation in CrmD.

After transfection/infection in BSC-1 cells, the intermediate single-crossover recombinant viruses in which the complete plasmid has been inserted into the ECTV genome were selected for three to five consecutive infection rounds in the presence of

puromycin and monitored for EGFP expression by fluorescence microscopy. Recombinant viruses (ECTVΔCrmD, ECTVRevCrmD, ECTVRevCRD and ECTVRevSECRET) were finally selected by successive plaque purification of white plaques in the absence of puromycin and screening with a *CrmD*-specific PCR. The complete genome sequence of ECTVRevCRD and ECTVRevSECRET was determined by Illumina sequencing to confirm the genomic structure and the absence of inadvertent mutations that may affect virus virulence[24]. The sequences have been submited to the European Nucleotide Archive and have been assigned reference number PRJEB19928. The number of sequencing reads that aligned with the ECTV Naval genome was 1,29 x 10^6 (93% of total sequencing reads) for ECTVRevCRD and 1,27 x 10^6 (87,4% of total sequencing reads) for ECTVRevSECRET. ECTVRevCRD was sequenced with a 325x coverage and, including the expected introduction of a truncated version of the duplicated *CrmD* gene, three changes were identified: Δ5.655-5.998 (*EVN006/CrmD* gene); T199.552C (*EVN200P* pseudogene) and Δ201.621-201.964 (*EVN201/CrmD* gene). ECTVRevSECRET was sequenced with a 320x coverage and, including the expected N77F mutation in the amino acid sequence of duplicated *CrmD* gene, three changes were identified: TT6.310-6.311AA (*EVN006/CrmD* gene); T199.552C (*EVN200P* pseudogene) and AA201.310-201.311TT (*EVN201/CrmD* gene). Both recombinant viruses had the expected mutations in both copies of the *CrmD* gene, present at the left and right ends of the viral genome. We also identified an additional point mutation in the inactive pseudogene EVN200P that was present in both ECTVRevCRD and ECTVRevSECRET, suggesting that this mutation was introduced during the generation of ECTVΔCrmD.

Infection of mice

621 Female BALB/c OlaHsd mice (6-8 weeks old) (Harlan), housed in ventilated racks,
622 were anesthesized with isofluorane and s.c. infected in the footpad with 10 µl of virus
623 inoculum. Viral doses were confirmed by titrating again on the same day the virus
624 dilutions used for mouse infections. Mice were housed in ventilated racks (Tecniplast)
625 under biological safety level 3 containment facilities. Monitoring of infected animals
626 was performed daily. Animals were weighed, scored for clinical signs of illness (scores
627 ranging from 0 for healthy animals to 4 for severely diseased animals) and footpad
628 swelling measured. Data analysis was performed using GraphPad Prism 6 (GraphPad
629 Software, La Jolla, CA, USA). Survival curves were compared using the Logrank
630 (Mantel-Cox) test. Footpad swelling and % initial weight data were analysed using
631 multiple t tests with false discovery rate Q=1%. Analyses were performed up to times
632 post-infection at which survival rates in the corresponding groups were above 50%.
633 ANOVA analyses with Bonferroni multiple comparison tests were performed in some
634 experiments, as indicated, for comparisons among groups and times post-infection at
635 which no mortalities were observed. These experiments were approved by the
636 Biological Safety Committee of the Centro de Investigación en Sanidad Animal (CISA,
637 INIA, Valdeolmos, Madrid) and animals were housed and handled according to legal
638 requirements.

639

640 **Immunohistochemistry and semiquantitative analyses**

641 Footpad, spleen and liver samples from infected mice were removed aseptically and
642 fixed in 10% buffered formalin solution to detect virus, ECTV CrmD protein and
643 chemokine receptors, and in zinc fixative (BDPharmingen) to detect lymphoid cells and
644 ICAM-1. After fixation, the samples were dehydrated through a graded series of alcohol

to xylol and embedded in paraffin wax. For structural and immunohistochemical analysis, sections (3 μm) were cut and stained with H&E or processed for immunohistochemical techniques. To detect virus and ECTV CrmD protein, formalin fixed serial sections were incubated with polyclonal rabbit anti-VACV antibody from a VACV-infected rabbit or a polyclonal rabbit anti-CrmD antibody against purified CrmD expressed in the baculovirus system. Both antibodies were generated in our laboratory. Secondary goat anti-rabbit IgG (Dako) was detected using an avidin-peroxidase-complex kit (PIERCE, Thermo Scientific) and 3,3´-diaminobenzidine tetrahydrochloride (Sigma) following the manufacturer´s instructions. The slides where counterstained with Mayer´s haematoxylin, dehydrated, and mounted with DPX mountant (Surgipath). Specific primary antibodies were replaced by PBS or normal goat serum in negative control sections. To detect lymphoid cells and chemokine receptors, the avidin-biotin alkaline-phosphatase staining method was used. Sections were dewaxed and immunostained with polyclonal rabbit anti-human CD3 (Dako), rat anti-mouse CD45R/B220, CD4, CD8a, and CD8b (BD Pharmingen) or goat anti-mouse CCR10 (AbCAM). Anti-mouse ICAM-1 antibody was from AbCAM. For CD3 and CCR10 immunohistochemistry, antigen retrieval was achieved by heating sections in 0.1 M citrate buffer at pH 6. Secondary goat anti-rabbit IgG, rabbit anti-rat IgG, or rabbit anti-goat IgG (Dako) were used as corresponded with the streptavidin-biotin-alkaline phosphatase kit (PIERCE, Thermo Scientific) and “FastRed” (Fast red sustrate packs, Lab Biogenex®) for detection of the immunogens, following the manufacturer’s indications. The slides were counterstained with Mayer’s haematoxylin, and mounted with Immu-mount (Thermo Shandon). Specific primary antibodies were replaced by PBS, normal rabbit serum or normal goat serum in negative control sections.

669 For semi-quantitative analyses of histological sections, samples from at least 5 animals
670 for each parameter were analysed in every case. To establish the degree of necrosis, a
671 minimum of 10 fields were scored per spleen and liver slice to obtain the mean value.
672 To quantify the morphological changes, sections were graded for necrosis using an
673 arbitrary scale: - negative findings (0 %); + slight (about 25 % necrosis); ++ moderate
674 (about 50 % necrosis); +++ very intense (about 90-100 % necrosis). Inflammatory
675 infiltration was evaluated in a minimum of 10 fields per liver slice or the complete
676 footpad section to obtain the mean value and it was scored as: - negative findings; +
677 slight; ++ moderate; +++ very intense. For antibody staining of lymphoid cells and
678 CCR10 chemokine receptor expressing cells, all the cells from the inflammatory
679 infiltrate were counted for each case and mean values are presented. In the case of anti-
680 ICAM-1 staining, all the blood vessels from sections from ECTV- (n = 5),
681 ECTVRevCrmD- (n = 5), and ECTVΔCrmD- (n = 6) infected mice were analysed and
682 scored as staining or non-staining. Mean percentage of staining vessels and standard
683 deviations were calculated using the Excel spreadsheet and statistical significance was
684 confirmed using a Student´s t-test ($p < 0.01$).

685

686 **Flow cytometry**

687 DPLN and spleens from PBS-inoculated or ECTV-infected BALB/c mice were
688 collected at 2 and 7 dpi, respectively, in RPMI supplemented with 10% FCS. Cell
689 suspensions were obtained by homogenization of the organs through 40 μm cell
690 strainers (BD Bioscience). Red blood cells were lysed by hypoosmotic shock in milli-Q
691 water and white cells were washed twice in PBS and counted manually in a
692 haemocytometer. DPLN cells were stained with anti-DX5-FITC (eBioscience), anti-

693 CD3e-PerCP (eBioscience) and anti-GzB-APC (R&D Biosystems). Splenocytes were
694 stained with anti-CD3e-PerCP, anti-CD8-PE (eBioscience) and anti-GzB-APC. In
695 parallel, cell suspensions were also stained with the appropriate isotype control
696 antibodies. 100,000 cells were analyzed in a FACS Calibur flow cytometer (Becton
697 Dickinson). Events were gated according to a forward and side scatter pattern
698 compatible with healthy lymphocytes (Supplementary Fig. 3). Results were analysed
699 with FlowJo software (FlowJo LLC).

700

701 **Immunization with recombinant purified ECTV CrmD**

702 A group of 15 female (6-8 week old) BALB/c mice was inoculated i.p. with 10 μg of
703 purified recombinant ECTV CrmD protein expressed in the baculovirus system per
704 animal three times at 17 to 20 d intervals. At 18 d after the last inoculation, mice were
705 bled and sera obtained to check for presence of anti-CrmD antibodies and challenged
706 s.c. with 1,000 PFU of ECTV as above. As a control, a group of 10 BALB/c mice was
707 subjected to the same protocol using PBS for i.p. inoculations and infected with equal
708 amounts of virus. Disease progression was monitored as described above.

709

710 **Data availability**

711 The data that support the findings of this study are available from the corresponding
712 author upon reasonable request. The viral genomic sequences reported have been
713 submited to the European Nucleotide Archive and have been assigned reference number
714 PRJEB19928 (www.ebi.ac.uk/ena/data/view/PRJEB19928).

715

716

717

718 **REFERENCES**

719 1. Alcami, A. Viral mimicry of cytokines, chemokines and their receptors. *Nat.*
720 *Rev. Immunol.* **3**, 36-50 (2003).
721 2. Epperson, M. L., Lee, C. A. & Fremont, D. H. Subversion of cytokine networks
722 by virally encoded decoy receptors. *Immunol. Rev.* **250**, 199-215 (2012).
723 3. Seet, B. T., Johnston, J. B., Brunetti, C. R., Barrett, J. W., Everett, H., Cameron,
724 C., Sypula, J., Nazarian, S. H., Lucas, A. & McFadden, G. Poxviruses and
725 immune evasion. *Annu. Rev. Immunol.* **21**, 377-423 (2003).
726 4. Felix, J. & Savvides, S. N. Mechanisms of immunomodulation by mammalian
727 and viral decoy receptors: insights from structures. *Nat. Rev. Immunol.* **17**,
728 112-129 (2017).
729 5. Smith, C. A., Hu, F. Q., Smith, T. D., Richards, C. L., Smolak, P., Goodwin, R. G.
730 & Pickup, D. J. Cowpox virus genome encodes a second soluble homologue
731 of cellular TNF receptors, distinct from CrmB, that binds TNF but not LT
732 alpha. *Virology* **223**, 132-147 (1996).
733 6. Smith, C. A., Davis, T., Wignall, J. M., Din, W. S., Farrah, T., Upton, C.,
734 McFadden, G. & Goodwin, R. G. T2 open reading frame from the Shope
735 fibroma virus encodes a soluble form of the TNF receptor. *Biochem. Biophys.*
736 *Res. Commun.* **176**, 335-342 (1991).
737 7. Saraiva, M., Smith, P., Fallon, P. G. & Alcami, A. Inhibition of type 1 cytokine-
738 mediated inflammation by a soluble CD30 homologue encoded by
739 ectromelia (mousepox) virus. *J. Exp. Med.* **196**, 829-839 (2002).
740 8. Saraiva, M. & Alcami, A. CrmE, a novel soluble tumor necrosis factor
741 receptor encoded by poxviruses. *J. Virol.* **75**, 226-233 (2001).
742 9. Rahman, M. M. & McFadden, G. Modulation of tumor necrosis factor by
743 microbial pathogens. *PLoS Pathog.* **2**, e4 (2006).
744 10. Panus, J. F., Smith, C. A., Ray, C. A., Smith, T. D., Patel, D. D. & Pickup, D. J.
745 Cowpox virus encodes a fifth member of the tumor necrosis factor receptor
746 family: a soluble, secreted CD30 homologue. *Proc. Natl. Acad. Sci. USA* **99**,
747 8348-8353 (2002).
748 11. Loparev, V. N., Parsons, J. M., Knight, J. C., Panus, J. F., Ray, C. A., Buller, R. M.,
749 Pickup, D. J. & Esposito, J. J. A third distinct tumor necrosis factor receptor of
750 orthopoxviruses. *Proc. Natl. Acad. Sci. USA* **95**, 3786-3791 (1998).
751 12. Hu, F. Q., Smith, C. A. & Pickup, D. J. Cowpox virus contains two copies of an
752 early gene encoding a soluble secreted form of the type II TNF receptor.
753 *Virology* **204**, 343-356 (1994).
754 13. Alejo, A., Pontejo, S. M. & Alcami, A. Poxviral TNFRs: properties and role in
755 viral pathogenesis. *Adv. Exp. Med. Biol.* **691**, 203-210 (2011).
756 14. Pontejo, S. M., Alejo, A. & Alcami, A. Poxvirus-encoded TNF decoy receptors
757 inhibit the biological activity of transmembrane TNF. *J. Gen. Virol.* **96**, 3118-
758 3123 (2015).

15. Pontejo, S. M., Alejo, A. & Alcami, A. Comparative Biochemical and Functional Analysis of Viral and Human Secreted Tumor Necrosis Factor (TNF) Decoy Receptors. *J. Biol. Chem.* **290**, 15973-15984 (2015).
16. Alejo, A., Ruiz-Arguello, M. B., Ho, Y., Smith, V. P., Saraiva, M. & Alcami, A. A chemokine-binding domain in the tumor necrosis factor receptor from variola (smallpox) virus. *Proc. Natl. Acad. Sci. USA* **103**, 5995-6000 (2006).
17. Heidarieh, H., Hernaez, B. & Alcami, A. Immune modulation by virus-encoded secreted chemokine binding proteins. *Virus Res.* **209**, 67-75 (2015).
18. Smith, G. L., Benfield, C. T., Maluquer de Motes, C., Mazzon, M., Ember, S. W., Ferguson, B. J. & Sumner, R. P. Vaccinia virus immune evasion: mechanisms, virulence and immunogenicity. *J. Gen. Virol.* **94**, 2367-2392 (2013).
19. Xue, X., Lu, Q., Wei, H., Wang, D., Chen, D., He, G., Huang, L., Wang, H. & Wang, X. Structural basis of chemokine sequestration by CrmD, a poxvirus-encoded tumor necrosis factor receptor. *PLoS Pathog.* **7**, e1002162 (2011).
20. Nelson, C. A., Epperson, M. L., Singh, S., Elliott, J. I. & Fremont, D. H. Structural Conservation and Functional Diversity of the Poxvirus Immune Evasion (PIE) Domain Superfamily. *Viruses* **7**, 4878-4898 (2015).
21. Sigal, L. J. The Pathogenesis and Immunobiology of Mousepox. *Adv. Immunol.* **129**, 251-276 (2016).
22. Esteban, D. J. & Buller, R. M. Ectromelia virus: the causative agent of mousepox. *J. Gen. Virol.* **86**, 2645-2659 (2005).
23. Chen, N., Danila, M. I., Feng, Z., Buller, R. M., Wang, C., Han, X., Lefkowitz, E. J. & Upton, C. The genomic sequence of ectromelia virus, the causative agent of mousepox. *Virology* **317**, 165-186 (2003).
24. Mavian, C., Lopez-Bueno, A., Bryant, N. A., Seeger, K., Quail, M. A., Harris, D., Barrell, B. & Alcami, A. The genome sequence of ectromelia virus Naval and Cornell isolates from outbreaks in North America. *Virology* **462-463**, 218-226 (2014).
25. Nolen, L. D., Osadebe, L., Katomba, J., Likofata, J., Mukadi, D., Monroe, B., Doty, J., Hughes, C. M., Kabamba, J., Malekani, J., Bomponda, P. L., Lokota, J. I., Balilo, M. P., Likafi, T., Lushima, R. S., Ilunga, B. K., Nkawa, F., Pukuta, E., Karhemere, S., Tamfum, J. J., Nguete, B., Wemakoy, E. O., McCollum, A. M. & Reynolds, M. G. Extended Human-to-Human Transmission during a Monkeypox Outbreak in the Democratic Republic of the Congo. *Emerg. Infec. Dis.* **22**, 1014-1021 (2016).
26. Shchelkunov, S. N. An increasing danger of zoonotic orthopoxvirus infections. *PLoS Pathog.* **9**, e1003756 (2013).
27. Stanford, M. M., McFadden, G., Karupiah, G. & Chaudhri, G. Immunopathogenesis of poxvirus infections: forecasting the impending storm. *Immunol. Cell. Biol.* **85**, 93-102 (2007).
28. Brady, G. & Bowie, A. G. Innate immune activation of NFkappaB and its antagonism by poxviruses. *Cytokine Growth Factor Rev.* **25**, 611-620 (2014).
29. Ruby, J., Bluethmann, H. & Peschon, J. J. Antiviral activity of tumor necrosis factor (TNF) is mediated via p55 and p75 TNF receptors. *J. Exp. Med.* **186**, 1591-1596 (1997).
30. Sambhi, S. K., Kohonen-Corish, M. R. & Ramshaw, I. A. Local production of tumor necrosis factor encoded by recombinant vaccinia virus is effective in

controlling viral replication in vivo. *Proc. Nat. Acad. Sci. USA* **88**, 4025-4029 (1991).
31. Nie, S., Cornberg, M. & Selin, L. K. Resistance to vaccinia virus is less dependent on TNF under conditions of heterologous immunity. *J. Immunol.* **183**, 6554-6560 (2009).
32. Chaudhri, G., Panchanathan, V., Buller, R. M., van den Eertwegh, A. J., Claassen, E., Zhou, J., de Chazal, R., Laman, J. D. & Karupiah, G. Polarized type 1 cytokine response and cell-mediated immunity determine genetic resistance to mousepox. *Proc. Natl. Acad. Sci. USA* **101**, 9057-9062 (2004).
33. Atrasheuskaya, A. V., Bukin, E. K., Fredeking, T. M. & Ignatyev, G. M. Protective effect of exogenous recombinant mouse interferon-gamma and tumour necrosis factor-alpha on ectromelia virus infection in susceptible BALB/c mice. *Clin. Exp. Immunol.* **136**, 207-214 (2004).
34. Chan, F. K., Shisler, J., Bixby, J. G., Felices, M., Zheng, L., Appel, M., Orenstein, J., Moss, B. & Lenardo, M. J. A role for tumor necrosis factor receptor-2 and receptor-interacting protein in programmed necrosis and antiviral responses. *J. Biol. Chem.* **278**, 51613-51621 (2003).
35. Palumbo, G. J., Buller, R. M. & Glasgow, W. C. Multigenic evasion of inflammation by poxviruses. *J. Virol.* **68**, 1737-1749 (1994).
36. Upton, C., Macen, J. L., Schreiber, M. & McFadden, G. Myxoma virus expresses a secreted protein with homology to the tumor necrosis factor receptor gene family that contributes to viral virulence. *Virology* **184**, 370-382 (1991).
37. Reading, P. C., Khanna, A. & Smith, G. L. Vaccinia virus CrmE encodes a soluble and cell surface tumor necrosis factor receptor that contributes to virus virulence. *Virology* **292**, 285-298 (2002).
38. Alcami, A., Khanna, A., Paul, N. L. & Smith, G. L. Vaccinia virus strains Lister, USSR and Evans express soluble and cell-surface tumour necrosis factor receptors. *J. Gen. Virol.* **80**, 949-959 (1999).
39. Alcami, A., Symons, J. A., Collins, P. D., Williams, T. J. & Smith, G. L. Blockade of chemokine activity by a soluble chemokine binding protein from vaccinia virus. *J. Immunol.* **160**, 624-633 (1998).
40. Zhou, Z., Connell, M. C. & MacEwan, D. J. TNFR1-induced NF-kappaB, but not ERK, p38MAPK or JNK activation, mediates TNF-induced ICAM-1 and VCAM-1 expression on endothelial cells. *Cell Signal.* **19**, 1238-1248 (2007).
41. Fang, M., Lanier, L. L. & Sigal, L. J. A Role for NKG2D in NK Cell-Mediated Resistance to Poxvirus Disease. *PLoS Pathog.* **4**, e30 (2008).
42. Fang, M. & Sigal, L. J. Direct CD28 costimulation is required for CD8+ T cell-mediated resistance to an acute viral disease in a natural host. *J. Immunol.* **177**, 8027-8036 (2006).
43. Mims, C. A. Aspects of the Pathogenesis of Virus Diseases. *Bacteriol. Rev.* **28**, 30-71 (1964).
44. Xu, R. H., Cohen, M., Tang, Y., Lazear, E., Whitbeck, J. C., Eisenberg, R. J., Cohen, G. H. & Sigal, L. J. The orthopoxvirus type I IFN binding protein is essential for virulence and an effective target for vaccination. *J. Exp. Med.* **205**, 981-992 (2008).
45. Rubio, D., Xu, R. H., Remakus, S., Krouse, T. E., Truckenmiller, M. E., Thapa, R. J., Balachandran, S., Alcami, A., Norbury, C. C. & Sigal, L. J. Crosstalk between

the type 1 interferon and nuclear factor kappa B pathways confers resistance to a lethal virus infection. *Cell Host Microbe* **13**, 701-710 (2013).
46. Schneider, K., Loewendorf, A., De Trez, C., Fulton, J., Rhode, A., Shumway, H., Ha, S., Patterson, G., Pfeffer, K., Nedospasov, S. A., Ware, C. F. & Benedict, C. A. Lymphotoxin-Mediated Crosstalk between B Cells and Splenic Stroma Promotes the Initial Type I Interferon Response to Cytomegalovirus. *Cell Host Microbe* **3**, 67-76 (2008).
47. Bartee, E., Mohamed, M. R., Lopez, M. C., Baker, H. V. & McFadden, G. The addition of tumor necrosis factor plus beta interferon induces a novel synergistic antiviral state against poxviruses in primary human fibroblasts. *J. Virol.* **83**, 498-511 (2009).
48. Gommerman, J. L., Browning, J. L. & Ware, C. F. The Lymphotoxin Network: orchestrating a type I interferon response to optimize adaptive immunity. *Cytokine Growth Factor Rev.* **25**, 139-145 (2014).
49. Parker, A. K., Parker, S., Yokoyama, W. M., Corbett, J. A. & Buller, R. M. Induction of natural killer cell responses by ectromelia virus controls infection. *J. Virol.* **81**, 4070-4079 (2007).
50. Cooper, M. A., Fehniger, T. A., Fuchs, A., Colonna, M. & Caligiuri, M. A. NK cell and DC interactions. *Trends Immunol.* **25**, 47-52 (2004).
51. Wehner, R., Dietze, K., Bachmann, M. & Schmitz, M. The bidirectional crosstalk between human dendritic cells and natural killer cells. *J. Innate Immunity* **3**, 258-263 (2011).
52. Andrews, D. M., Scalzo, A. A., Yokoyama, W. M., Smyth, M. J. & Degli-Esposti, M. A. Functional interactions between dendritic cells and NK cells during viral infection. *Nat. Immunol.* **4**, 175-181 (2003).
53. Kaminsky, L. W., Sei, J. J., Parekh, N. J., Davies, M. L., Reider, I. E., Krouse, T. E. & Norbury, C. C. Redundant Function of Plasmacytoid and Conventional Dendritic Cells Is Required To Survive a Natural Virus Infection. *J. Virol.* **89**, 9974-9985 (2015).
54. Xu, J., Chakrabarti, A. K., Tan, J. L., Ge, L., Gambotto, A. & Vujanovic, N. L. Essential role of the TNF-TNFR2 cognate interaction in mouse dendritic cell-natural killer cell crosstalk. *Blood* **109**, 3333-3341 (2007).
55. Tufa, D. M., Chatterjee, D., Low, H. Z., Schmidt, R. E. & Jacobs, R. TNFR2 and IL-12 coactivation enables slanDCs to support NK-cell function via membrane-bound TNF-alpha. *Eur. J. Immunol.* **44**, 3717-3728 (2014).
56. Hickman, H. D., Reynoso, G. V., Ngudiankama, B. F., Cush, S. S., Gibbs, J., Bennink, J. R. & Yewdell, J. W. CXCR3 chemokine receptor enables local CD8(+) T cell migration for the destruction of virus-infected cells. *Immunity* **42**, 524-537 (2015).
57. Kagami, S., Saeki, H., Komine, M., Kakinuma, T., Nakamura, K., Tsunemi, Y., Sasaki, K., Asahina, A. & Tamaki, K. CCL28 production in HaCaT cells was mediated by different signal pathways from CCL27. *Exp. Dermatol.* **15**, 95-100 (2006).
58. Homey, B., Alenius, H., Muller, A., Soto, H., Bowman, E. P., Yuan, W., McEvoy, L., Lauerma, A. I., Assmann, T., Bunemann, E., Lehto, M., Wolff, H., Yen, D., Marxhausen, H., To, W., Sedgwick, J., Ruzicka, T., Lehmann, P. & Zlotnik, A. CCL27-CCR10 interactions regulate T cell-mediated skin inflammation. *Nat. Med.* **8**, 157-165 (2002).

59. Gileva, I. P., Viazovaia, E. A., Toporkova, L. B., Tsyrendorzhiev, D. D., Shchelkunov, S. N. & Orlovskaya, I. A. TNF binding protein of variola virus acts as a TNF antagonist at epicutaneous application. *Curr. Pharm. Biotechnol.* **16**, 72-76 (2015).
60. Katzman, S. D. & Fowell, D. J. Pathogen-imposed skewing of mouse chemokine and cytokine expression at the infected tissue site. *J. Clin. Invest.* **118**, 801-811 (2008).
61. Serbina, N. V., Salazar-Mather, T. P., Biron, C. A., Kuziel, W. A. & Pamer, E. G. TNF/iNOS-producing dendritic cells mediate innate immune defense against bacterial infection. *Immunity* **19**, 59-70 (2003).
62. Salazar-Mather, T. P. & Hokeness, K. L. Cytokine and chemokine networks: pathways to antiviral defense. *Curr. Top. Microbiol. Immunol.* **303**, 29-46 (2006).
63. Rubins, K. H., Hensley, L. E., Jahrling, P. B., Whitney, A. R., Geisbert, T. W., Huggins, J. W., Owen, A., Leduc, J. W., Brown, P. O. & Relman, D. A. The host response to smallpox: analysis of the gene expression program in peripheral blood cells in a nonhuman primate model. *Proc. Natl. Acad. Sci. USA* **101**, 15190-15195 (2004).
64. Gileva, I. P., Nepomnyashchikh, T. S., Antonets, D. V., Lebedev, L. R., Kochneva, G. V., Grazhdantseva, A. V. & Shchelkunov, S. N. Properties of the recombinant TNF-binding proteins from variola, monkeypox, and cowpox viruses are different. *Biochim. Biophys. Acta* **1764**, 1710-1718 (2006).
65. Parrino, J. & Graham, B. S. Smallpox vaccines: Past, present, and future. *J. Allergy Clin. Immunol.* **118**, 1320-1326 (2006).
66. Gilchuk, I., Gilchuk, P., Sapparapu, G., Lampley, R., Singh, V., Kose, N., Blum, D. L., Hughes, L. J., Satheshkumar, P. S., Townsend, M. B., Kondas, A. V., Reed, Z., Weiner, Z., Olson, V. A., Hammarlund, E., Raue, H. P., Slifka, M. K., Slaughter, J. C., Graham, B. S., Edwards, K. M., Eisenberg, R. J., Cohen, G. H., Joyce, S. & Crowe, J. E., Jr. Cross-Neutralizing and Protective Human Antibody Specificities to Poxvirus Infections. *Cell* **167**, 684-694 e689 (2016).
67. Xiao, Y., Aldaz-Carroll, L., Ortiz, A. M., Whitbeck, J. C., Alexander, E., Lou, H., Davis, H. L., Braciale, T. J., Eisenberg, R. J., Cohen, G. H. & Isaacs, S. N. A protein-based smallpox vaccine protects mice from vaccinia and ectromelia virus challenges when given as a prime and single boost. *Vaccine* **25**, 1214-1224 (2007).
68. Heraud, J. M., Edghill-Smith, Y., Ayala, V., Kalisz, I., Parrino, J., Kalyanaraman, V. S., Manischewitz, J., King, L. R., Hryniewicz, A., Trindade, C. J., Hassett, M., Tsai, W. P., Venzon, D., Nalca, A., Vaccari, M., Silvera, P., Bray, M., Graham, B. S., Golding, H., Hooper, J. W. & Franchini, G. Subunit recombinant vaccine protects against monkeypox. *J. Immunol.* **177**, 2552-2564 (2006).
69. Xu, R. H., Rubio, D., Roscoe, F., Krouse, T. E., Truckenmiller, M. E., Norbury, C. C., Hudson, P. N., Damon, I. K., Alcami, A. & Sigal, L. J. Antibody inhibition of a viral type 1 interferon decoy receptor cures a viral disease by restoring interferon signaling in the liver. *PLoS Pathog.* **8**, e1002475 (2012).
70. Feldmann, M. & Maini, R. N. Anti-TNF alpha therapy of rheumatoid arthritis: what have we learned? *Annu. Rev. Immunol.* **19**, 163-196 (2001).
71. Fallon, P. G. & Alcami, A. Pathogen-derived immunomodulatory molecules: future immunotherapeutics? *Trends Immunol.* **27**, 470-476 (2006).

952 72. Viejo-Borbolla, A., Martin, A. P., Muniz, L. R., Shang, L., Marchesi, F.,
953 Thirunarayanan, N., Harpaz, N., Garcia, R. A., Apostolaki, M., Furtado, G. C.,
954 Mayer, L., Kollias, G., Alcami, A. & Lira, S. A. Attenuation of TNF-driven
955 murine ileitis by intestinal expression of the viral immunomodulator CrmD.
956 *Mucosal Immunol.* **3**, 633-644 (2010).
957 73. Ali, T., Kaitha, S., Mahmood, S., Ftesi, A., Stone, J. & Bronze, M. S. Clinical use
958 of anti-TNF therapy and increased risk of infections. *Drug Healthc. Patient*
959 *Saf.* **5**, 79-99 (2013).
960 74. Alejo, A., Saraiva, M., Ruiz-Arguello, M. B., Viejo-Borbolla, A., de Marco, M. F.,
961 Salguero, F. J. & Alcami, A. A method for the generation of ectromelia virus
962 (ECTV) recombinants: in vivo analysis of ECTV vCD30 deletion mutants.
963 *PloS ONE* **4**, e5175 (2009).

964

965 ACKNOWLEDGEMENTS

966 We thank Javier Salguero for help with animal experimentation and
967 immunohistochemistry, Rocío Martín and Carolina Sánchez for technical assistance and
968 Daniel Rubio for discussions on the project. This work was funded by Grants from the
969 Spanish Ministry of Economy and Competitiviness and European Union (European
970 Regional Development's Funds, FEDER) (grant SAF2015-67485-R), and the Wellcome
971 Trust (grant 051087/Z97/Z). M. B. R.-A. and A. Alejo were recipients of a Ramón y
972 Cajal Contract from the Spanish Ministry of Science and Innovation.

973

974 AUTHOR CONTRIBUTIONS

975 A. Alejo, M. B. R.-A. and A. Alcami conceived and designed the research; A. Alejo, M.
976 B. R.-A. and S. M. P. performed most of the experiments; M. S. contributed to the
977 construction of recombinant viruses; B. H. performed the genome sequence analysis of
978 recombinant viruses; M. M. F. M. provided support for animal experiments and carried
979 out histology and immunohistochemistry analyses. A. Alejo, M. B. R.-A. S. M. P. and

A. Alcami wrote the manuscript. All authors discussed the results and commented on the manuscript.

COMPETING INTERESTS

The authors declare no competing i nterests.

985 **LEGENDS TO FIGURES**

986

987 **Figure 1. ECTV CrmD recombinant viruses**

988 (a) Schematic diagram of the genomic structure of the recombinant ECTVs generated
989 for the study of the role of ECTV CrmD in mousepox pathogenesis. The names of the
990 genes flanking the *CrmD* locus are indicated. In grey, the *CrmD* locus in the parental
991 and recombinant viruses is shown. Both left Inverted Terminal Repeat (lITR) and right
992 ITR (rITR) are represented for ECTV, whereas the lITR is shown for the other viruses.
993 (b) Western blot analyses using anti-CrmD and anti-35-kDa vCKBP antisera of
994 supernatants from BSC-1 cells that were mock-infected (1) or infected with ECTV (2),
995 ECTVΔCrmD (3), ECTVRevCrmD (4) or ECTVRevCRD (5) at a multiplicity of
996 infection of 5 PFU/cell and harvested at 24 h post-infection. The position of the
997 respective proteins is indicated by arrows. Molecular size markers in kDa are shown on
998 the left. (c) TNF-induced cytotoxicity assay. Increasing amounts of recombinant ECTV
999 CrmD (rCrmD, in μg/ml) or supernatants (equivalent to 5, 10 or 30 x 10^3 cells) obtained
1000 as in panel B were added to block the effect of TNF on L929 cells. The values obtained
1001 in the presence of mock-infected cell supernatants have been substracted in each case.
1002 Data are mean + / - standard error of the mean (SEM) of triplicate samples. (d) Single-
1003 step growth curves of the indicated viruses. BSC-1 cells were infected with 5 PFU/cell
1004 and the virus production was titrated at the indicated h post-infection. The means of
1005 duplicate samples are shown.

1006

1007

Figure 2. Mousepox pathogenesis in the absence of ECTV CrmD

Groups of 10 (left panels) or 5 (right panels) BALB/c mice were inoculated s.c. in the left hind footpad with 10 PFU or 1,000 PFU, respectively, of ECTV (○), ECTVΔCrmD (▲), ECTVRevCrmD (●), ECTVRevCRD (△) or PBS alone (■), and monitored daily for weight loss, signs of illness and footpad swelling, as indicated. Data are shown as mean + / - SEM. Statistical analyses were performed using multiple t-tests with false discovery rate at Q=1%. Analyses were performed up to times post infection at which survival rates in the corresponding group were above 50%. Black bars indicate time points at which significant differences ($p < 0.01$) between ECTV- / ECTVRevCrmD- and ECTVΔCrmD-inoculated mice were found. Asterisks indicate time points at which significant differences ($p < 0.01$) between ECTVΔCrmD and ECTVRevCRD-inoculated mice were found. The bottom panels show the number of surviving animals during the course of infection. Data are from one experiment representative of three independent experiments.

Figure 3. Inflammatory response in the footpad of ECTVΔCrmD-infected mice

Left hind foot (a, b) and H&E staining (c, d) and anti-ICAM-1 staining (e, f) of zinc-fixed footpad sections of representative BALB/c mice infected with 1,000 PFU of ECTV (a, c, e) or ECTVΔCrmD (b, d, f) at 7 dpi. Anti-CD4 staining (g) of zinc-fixed and anti-CCR10 staining (h) of formalin-fixed footpad sections of representative ECTVΔCrmD-infected mice are shown. No cell infiltrate was observed in the ECTV-infected tissues. For all immunohistochemistry analyses, postively labelled cells appear in red colour. Scale bar, 100 µm (c-f) and 25 µm (g, h).

Figure 4. CrmD binding affinity for mouse chemokines. (a) Binding screening of mouse chemokines to CrmD. Recombinant CrmD was immobilized on a CM4 SPR biosensor chip at 1500 RU. Chemokines (100 nM) were injected at 10 µl/min flow rate in HBS-EP buffer. Binding was monitored during 180 s followed by a 120 s dissociation periods. (b) Binding kinetic constants -Ka (association), Kd (dissociation) and KD (affinity)- and their corresponding SEM for the CrmD interaction with some of its chemokine ligands. For affinity determination purposes, CrmD was immobilized on a CM4 SPR biosensor chip at 900 RUs. The binding of increasing concentrations of chemokine (1-50 nM), injected at a 30 µl/min flow rate, was recorded during 120 s followed by a 300 s dissociation. Binding curves were fitted according to a 1:1 Langmuir model. (c) Two examples of affinity determination fittings are shown.

Figure 5. Impaired virus spread in the absence of ECTV CrmD

Graphs show viral titres at 3, 7 and 11 dpi in spleen (a) and liver (b) of BALB/c mice infected with 1,000 PFU per animal of the indicated viruses. Data are mean log +/- SEM of groups of 5 animals for each condition. Note that mice infected with ECTV or ECTVRevCrmD did not survive to 11 dpi. Left hind foot anti-poxvirus staining (c-e) or anti-CrmD staining (f-h) of zinc-fixed footpad sections of representative BALB/c mice infected with 1,000 PFU of ECTVRevCrmD (c, f), ECTVΔCrmD (d, g) or ECTVRevCRD (e, h) at 7 dpi. H&E staining of spleen (i-k) or liver (l-n) sections of representative mice infected with 1,000 PFU of ECTVRevCrmD (i, l), ECTVΔCrmD (j, m) or ECTVRevCRD (k, n) at 7 dpi. Insets show enlargement of selected areas to illustrate necrosis (l, n) and inflammatory infiltrate (m). Data are from one experiment

representative of two independent experiments. Scale bar, 100 µm (c-k) and 40 µm (l-n).

Figure 6. CrmD N77F mutant blocks chemokines but lacks anti-TNF activity

(a) Coomasie blue stained gel showing 500 ng of recombinant CrmD wild type (WT) and N77F mutant expressed by recombinant baculoviruses. Molecular mass standards are shown in kDa. (b) CrmD N77F binds mouse Ccl25 but not mouse TNF (mTNF). The binding of 100 nM Ccl25 and mTNF to CrmD WT or N77F mutant was assessed by SPR experiments. (c) CrmD N77F mutant does not interfere with mouse TNF-mediated cytotoxicity on L929 cells. The cell viability of L929 cells after a 18 h incubation with 1.2 nM TNF in the absence or presence of the indicated molar ratios of CrmD variants was determined. Data is represented as mean ± standard deviation (SD) of the % relative to cells incubated without TNF (media). (d) CrmD N77F blocks mouse Ccl25-induced migration of MOLT-4 cells. The number of cells that migrated through the transwell filter after 4 h incubation at 37^{o}C with 50 nM mouse Ccl25 in the absence or presence of the indicated increasing molar ratios of CrmD variants is shown. Data is represented as mean ± SD of triplicates. In c and d, one experiment representative of three independent experiments is shown.

Figure 7. The activity of the SECRET domain *in vivo* is dependent on concomitant TNF blockade

(a) Schematic diagram of the genomic structure of ECTV RevSECRET. The genes flanking the *CrmD* locus are indicated. In grey, the *CrmD* locus in the parental and

recombinant virus is shown. Presence of a point mutation (N77F) in the CrmD of ECTVRevSECRET is indicated by an asterisk and a black line. Only the left Inverted Terminal Repeat is shown. (b) Western blot analyses using anti-CrmD and anti-35-kDa vCKBP antisera of supernatants from BSC-1 cells mock-infected (1) or infected with ECTVΔCrmD (2), ECTVRevCrmD (3), ECTVRevCRD (4) or ECTVRevSECRET (5) at a multiplicity of infection of 5 PFU/cell and harvested at 24 h post-infection. The position of the proteins is indicated by arrows. Molecular size markers in kDa are shown on the left. (c) TNF-induced cytotoxicity assay. Increasing amounts of supernatants (equivalent to 2, 8 or 16 x 10^3 cells) from cells infected with the indicated viruses were added to block the effect of TNF on L929 cells. Values of % cell viability obtained in the presence of mock-infected cell supernatants were subtracted from the % cell viability caused by the corresponding supernatant volume from virus-infected cells. Data are mean +/- SD of triplicate samples. (d) Mortality rate determination of CrmD recombinant ECTVs in susceptible mice. Groups of 5 or 10 female BALB/c mice were infected s.c. in the left hind footpad with different doses of the indicated viruses. The number of survivors at 15 dpi and the mean time to death (MTD) in days for each condition are shown. n.a., not applicable. (e) Groups of 5 female BALB/c mice were inoculated s.c. in the left hind footpad with 10^6 PFU of ECTV RevCrmD (●), ECTVΔCrmD (▲), ECTVRevCRD (△) or ECTVRevSECRET (□) and monitored daily for mortality and footpad swelling, as indicated. Data are shown as mean +/- SD. Asterisks indicate time points at which significant differences ($p < 0.01$, multiple t tests with false discovery rate correction at Q=1%) between ECTVΔCrmD and ECTVRevSECRET-inoculated mice were found. (f) Replication of recombinant ECTVs in spleen. Viral titres at 7 dpi in spleen of mice infected with 10^5 PFU per animal of the indicated viruses. Data are mean log +/- SD of groups of 5 mice for each condition.

1103 Groups significantly different from the ECTVRevCrmD-infected group are indicated
1104 (asterisks $p<0.05$, ANOVA with Bonferroni multiple comparison test).

1105

1106 **Figure 8. Inhibition of TNF activity *in vivo* impairs NK cell activation in response**
1107 **to ECTV infection**

1108 Cells from DPLN (a, b, c, d) harvested at 2 dpi or from spleens (a, e, f) collected at 7
1109 dpi from PBS-inoculated BALB/c mice or mice infected with 10^5 pfu of the indicated
1110 viruses were analyzed by flow cytometry using conjugated anti-CD3, anti-CD8, anti-
1111 DX5 and anti-granzyme B (GzB) antibodies. In A, representative dot plots of the
1112 staining of NK cells (CD3- DX5+; top panel) and CD8 T cells (CD3+ CD8+; bottom
1113 panel) isolated from DPLN or spleen, respectively, are shown. Number inside each
1114 graph indicates the % of cells inside the depicted gates. In b and c, a quantification of
1115 the total number and % of NK cells, respectively, is presented. The % of NK cells
1116 expressing granzyme B in each group is quantified in d. In e and f, a quantification of
1117 the total number of CD8 T cells and granzyme B-expressing CD8 T cells detected for
1118 each group is shown. The number of events positively stained with the corresponding
1119 isotype control antibodies (isotype DX5, 0.15% positives; isotype CD8, 1.3% positives;
1120 isotype granzyme B, 0.02% and 0.03% positives in DPLN and spleen, respectively)
1121 were subtracted from each sample for the quantification analyses. Data are mean +/- SD
1122 from one experiment representative of three independent experiments with 4-5 animals
1123 per group. Statistically significant groups are indicated (asterisks $p<0.05$, ANOVA with
1124 Bonferroni multiple comparison test).

1125

Figure 9. Immunization with purified recombinant ECTV CrmD protects mice from fatal mousepox

Groups of BALB/c mice were immunized with PBS (n = 10) (PBS, open circle) or recombinant ECTVCrmD protein (n = 15) (rCrmD, close triangle), and challenged with 1,000 PFU of ECTV per animal at 18 d after concluding the immunization procedure. (a) Neutralization of TNF activity in a TNF-induced cytotoxicity assay by serum from mice immunized with CrmD or PBS. L929 cells were incubated with TNF and CrmD in the presence of 1 µl (open bars) or 2 µl (close bars) of serum from mice immunized with CrmD (CrmD 1-15) or PBS (PBS 1-2). As controls, cell viability was determined in the absence of TNF (no TNF) or in the presence of TNF (TNF) incubated also with CrmD (TNF CrmD) or an antiserum against CrmD (anti CrmD). Mice that succumbed to infection are indicated with a cross. Data are mean +/- SEM of triplicate samples. Mice infected with ECTV were monitored for weight loss (b), signs of illness (c), footpad swelling (d) and mortality (e) at the indicated times of infecion. Data are shown as mean +/- SEM.

Table 1: Mortality rate determination of CrmD recombinant ECTVs in susceptible BALB/c mice

Dose (pfu)	ECTV		ECTV RevCrmD		ECTV ΔCrmD		ECTV RevCRD	
	survivors	MTD	survivors	MTD	survivors	MTD	survivors	MTD
10	4/10	10.0 (9-11)	0/10	11.6 (9-21)	10/10	n.a.	10/10	n.a.
10e2	0/5	11.8 (9-18)	1/5	12.8 (10-11)	5/5	n.a.	5/5	n.a.
10e3	0/5	10.4 (9-14)	0/5	10.2 (9-13)	5/5	n.a.	4/5	10
10e4	n.d.	n.d.	0/5	8.6 (8-10)	5/5	n.a.	5/5	n.a.
10e5	n.d.	n.d.	0/5	9.6 (8-13)	5/5	n.a.	3/5	9 (8-10)
10e6	n.d.	n.d.	n.d.	n.d.	5/5	n.a.	n.d.	n.d.
10e7	n.d.	n.d.	n.d.	n.d.	4/5	14	1/5	12.5 (10-16)

Groups of 5 or 10 BALB/c female mice were infected s.c. in the left hind footpad with different doses of the indicated viruses. The number of survivors at 32 dpi and the mean time to death (MTD) and survival range (in parenthesis) in d for each condition are shown. n.a., not applicable; n.d., not determined.

Table 2: Histopathology of spleen and liver in recombinant ECTV-infected mice

	3 dpi		7 dpi		11 dpi	
	spleen[a]	liver[a / b]	spleen[a]	liver[a / b]	spleen[a]	liver[a / b]
EV	-	- / -	+++	+ / +	n.a.	n.a.
EV RevCrmD	-	- / -	+++	+ / +	n.a.	n.a.
EV ΔCrmD	-	- / -	+	- / ++	+	- / ++
EV RevCRD	-	- / -	++	+ / +	+	- / ++

Groups of 5 BALB/c mice were infected s.c. in the left hind footpad with the indicated viruses and sacrificed at different dpi. Spleen and liver were H&E-stained for histopathological analysis. Degree of necrosis[a] was semiquantitatively assessed using an arbitrary scale: - negative findings (0 %); + slight (about 25 % necrosis); ++ moderate (about 50 % necrosis); +++ very intense (about 90-100 % necrosis). Presence of inflammatory infiltrate[b] was evaluated in a minimum of 10 fields per liver slice section to obtain the mean value and it was scored as: - negative findings; + slight; ++ moderate; +++ very intense. n.a. not applicable.

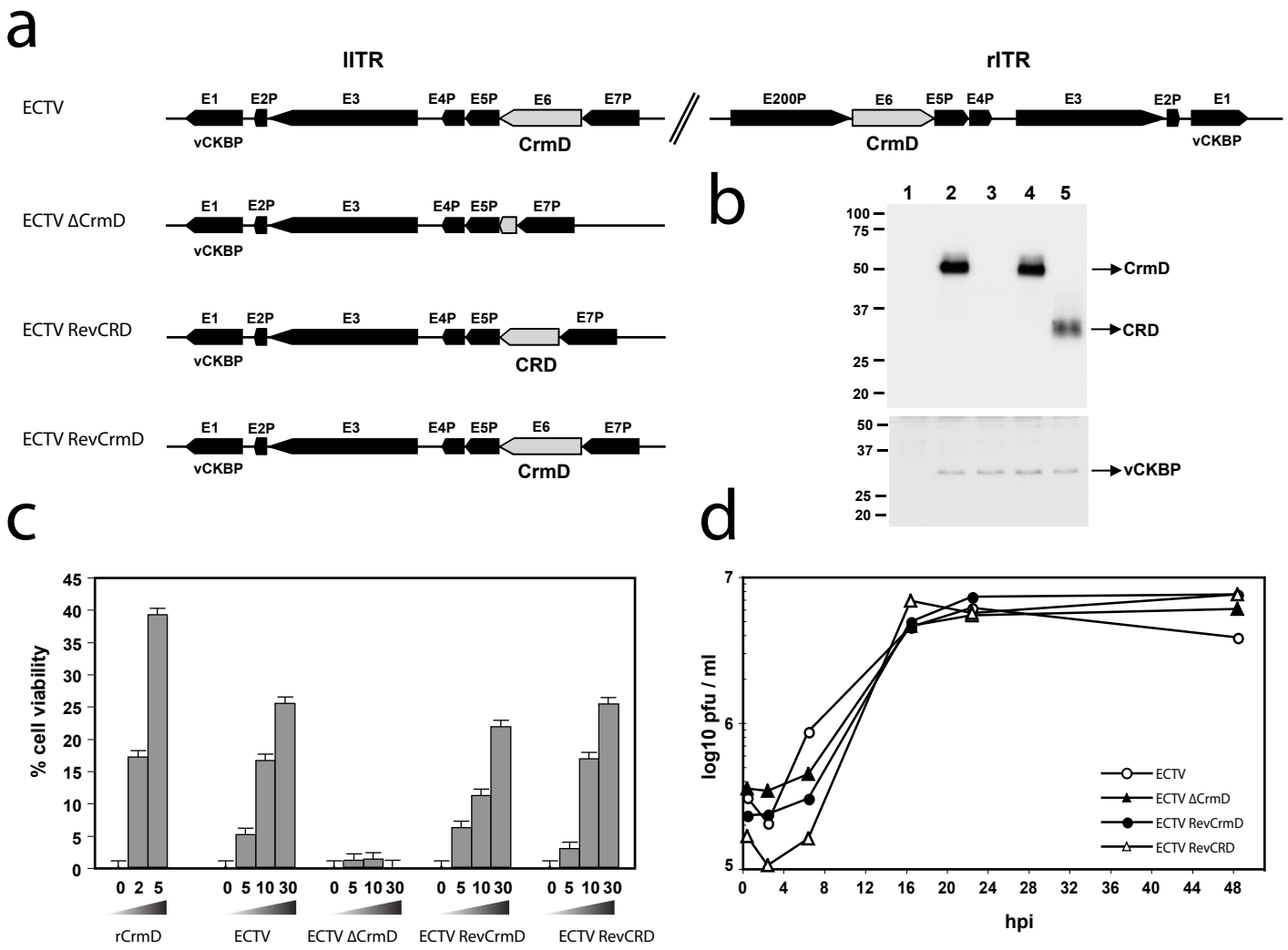
a
lITR
rITR
ECTV
E1 E2P E3 E4P E5P E6 E7P
vCKBP
CrmD
E200P E6 E5P E4P E3 E2P E1
ECTV ΔCrmD
E1 E2P E3 E4P E5P E7P
ECTV RevCRD
CRD
ECTV RevCrmD
b
1 2 3 4 5
100
75
50
37
25
20
CrmD
CRD
vCKBP
c
% cell viability
0 2 5
0 5 10 30
rCrmD
ECTV
ECTV ΔCrmD
ECTV RevCrmD
ECTV RevCRD
d
log10 pfu / ml
hpi
ECTV
ECTV ΔCrmD
ECTV RevCrmD
ECTV RevCRD

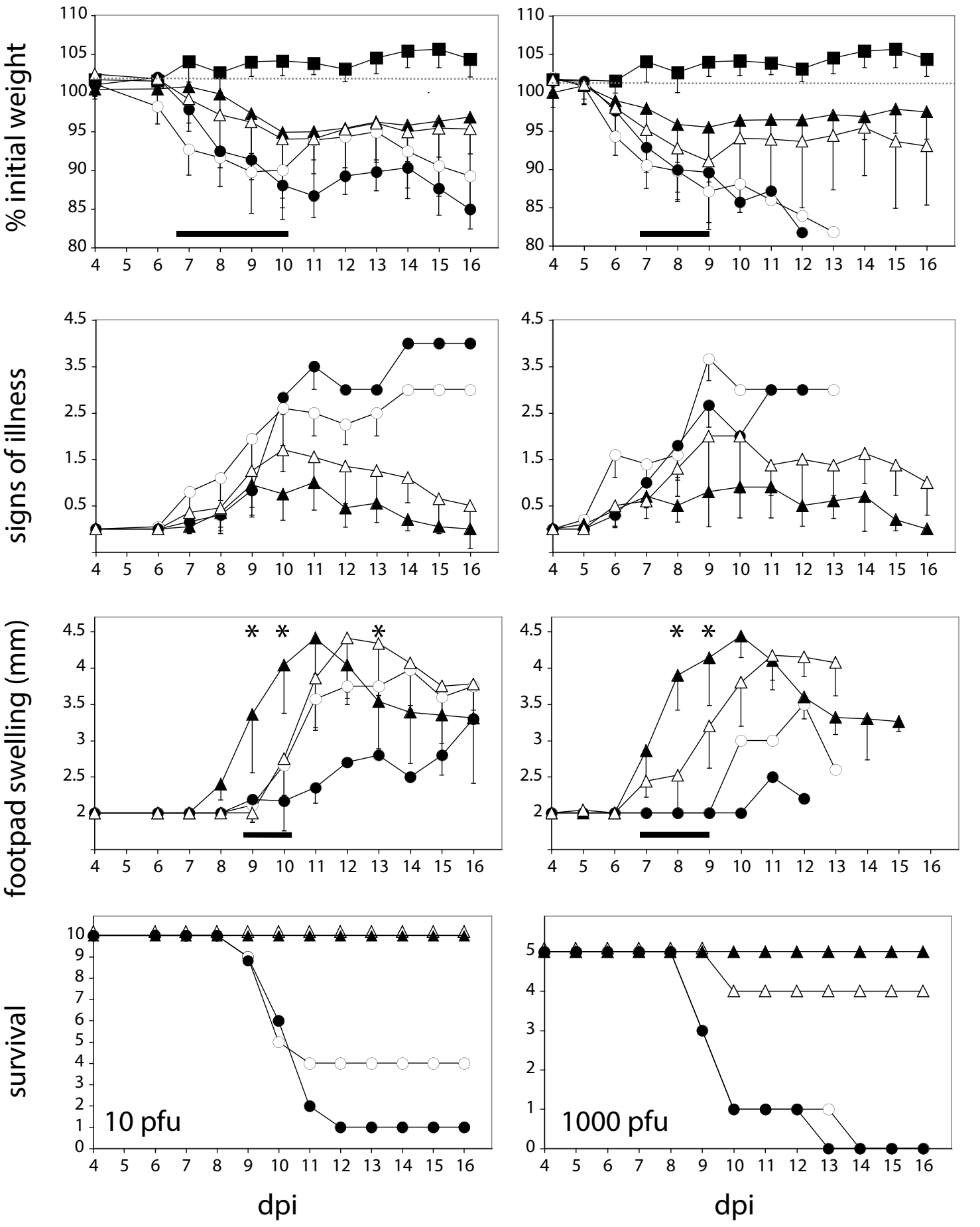
% initial weight
signs of illness
footpad swelling (mm)
survival
10 pfu
1000 pfu
dpi
dpi

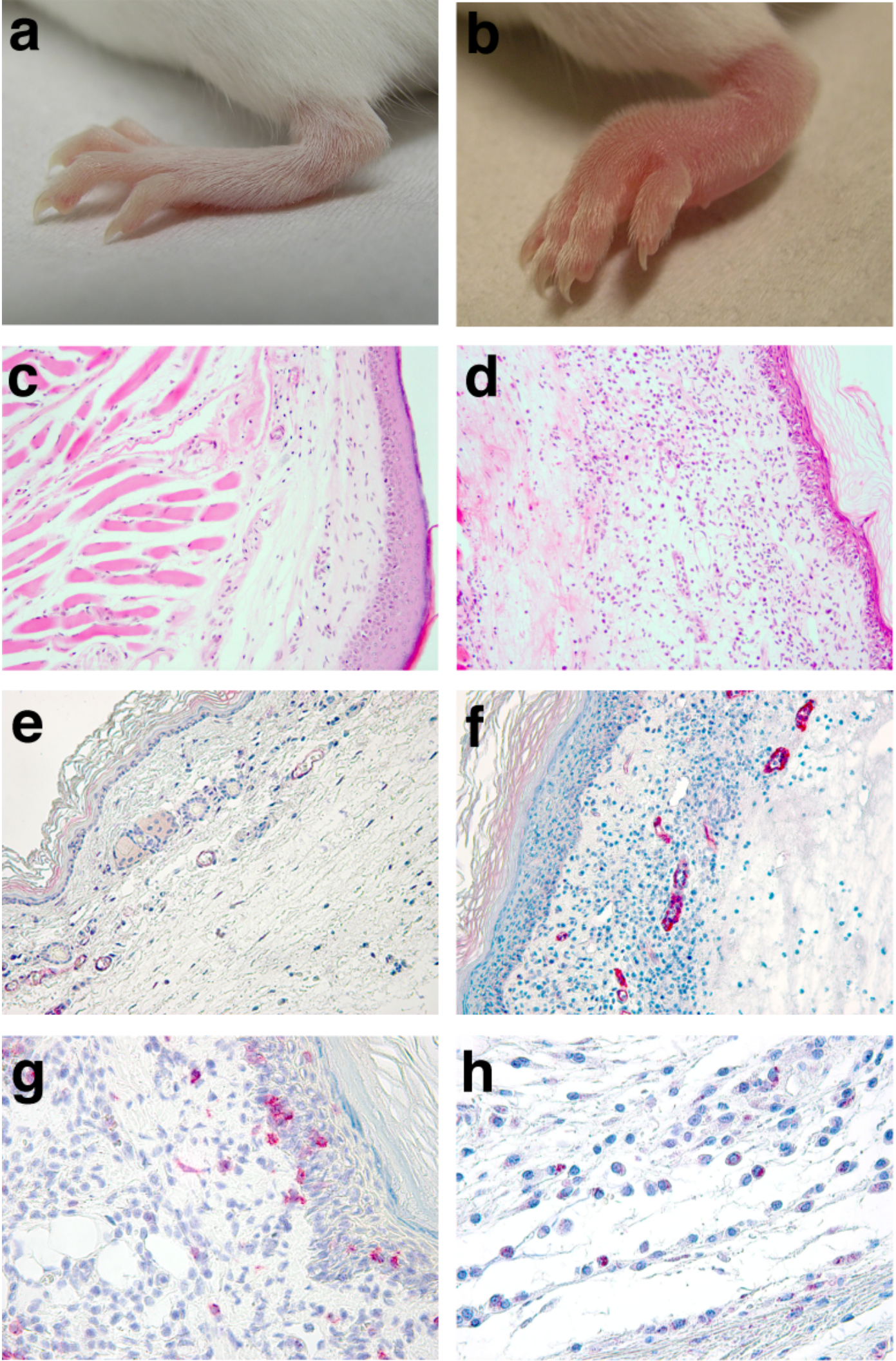
a
b
c
d
e
f
g
h

a

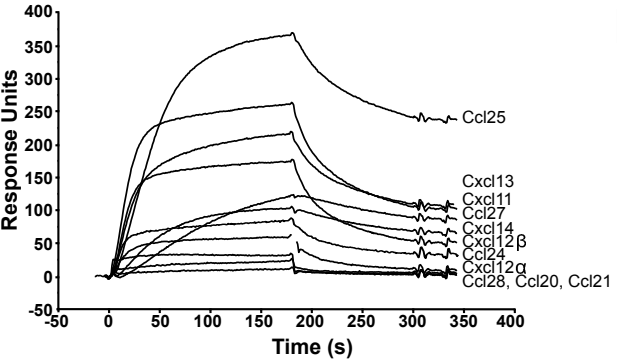

b

Chemokine	Ka (SE) (1/Ms)	Kd (SE) (1/s)	K_D (nM)
Ccl24	3.18×10^5 (5.00×10^3)	2.87×10^{-3} (4.50×10^{-5})	**9.00**
Ccl25	4.05×10^5 (2.25×10^3)	1.97×10^{-3} (2.11×10^{-5})	**4.86**
Ccl27	6.89×10^5 (1.32×10^4)	3.72×10^{-3} (3.69×10^{-5})	**5.41**
Cxcl11	4.96×10^5 (1.20×10^3)	2.42×10^{-3} (2.75×10^{-5})	**4.87**
Cxcl12β	5.61×10^5 (1.24×10^4)	9.31×10^{-3} (6.56×10^{-5})	**16.60**
Cxcl13	1.61×10^5 (4.82×10^3)	2.12×10^{-3} (3.18×10^{-5})	**13.20**
Cxcl14	1.02×10^6 (8.10×10^4)	4.10×10^{-2} (2.70×10^{-3})	**40.20**

c

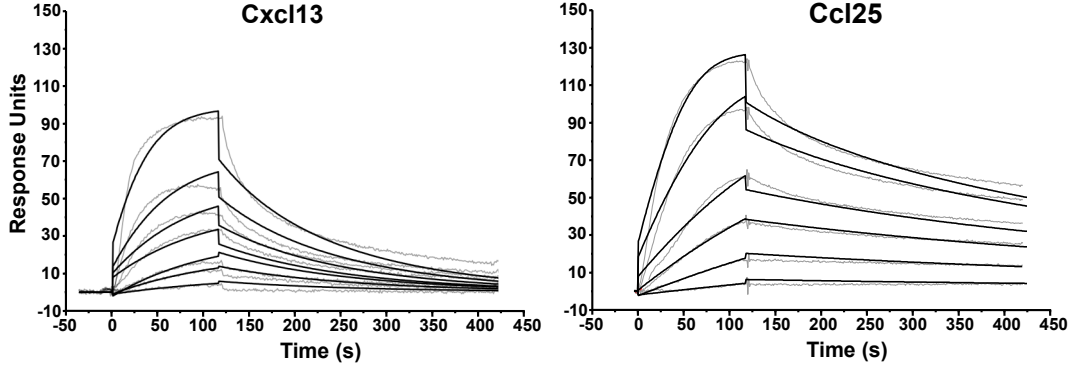

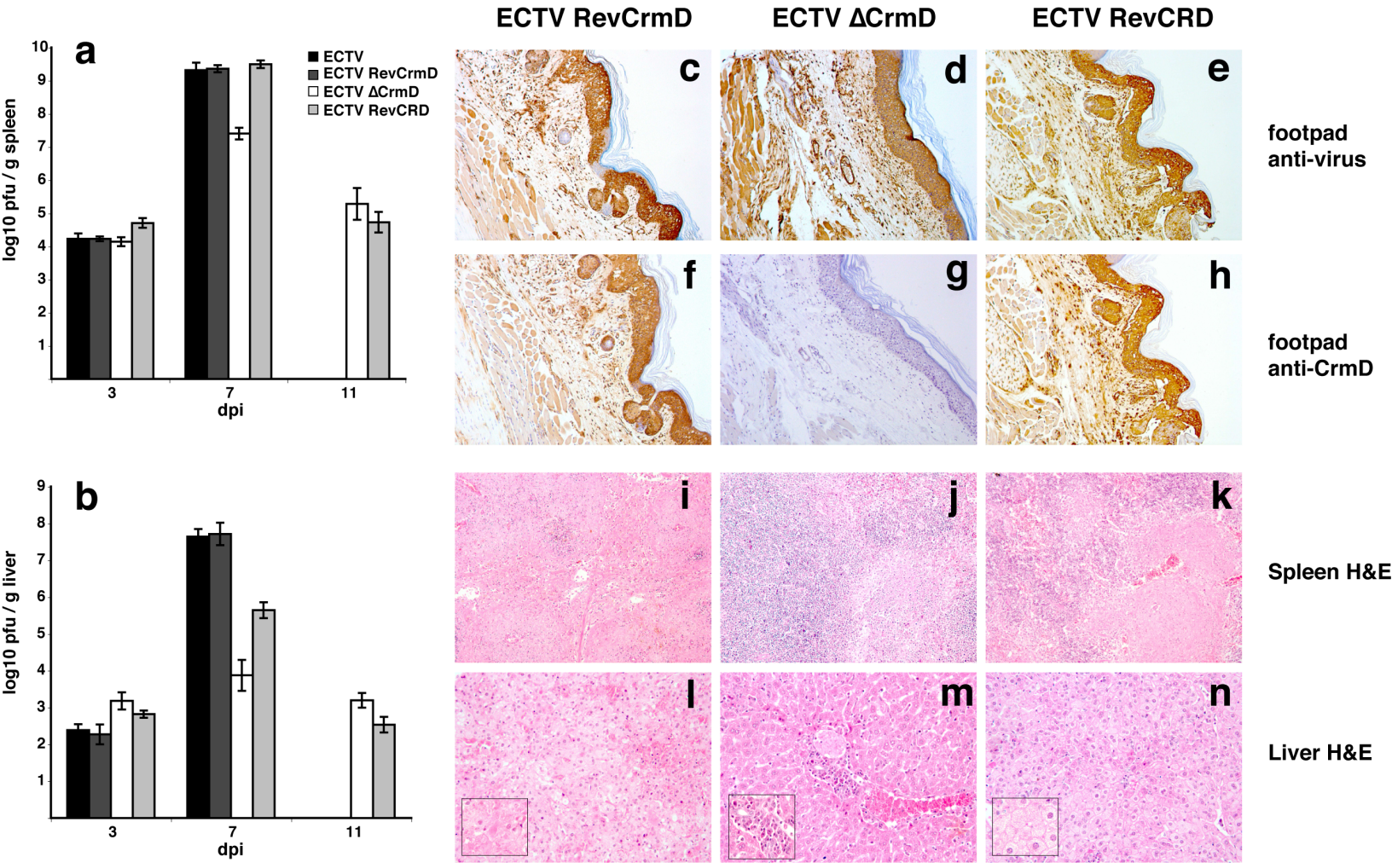
a
log10 pfu / g spleen
10
9
8
7
6
5
4
3
2
1
3
7
11
dpi
ECTV
ECTV RevCrmD
ECTV ΔCrmD
ECTV RevCRD
b
log10 pfu / g liver
9
8
7
6
5
4
3
2
1
3
7
11
dpi
ECTV RevCrmD
ECTV ΔCrmD
ECTV RevCRD
c
d
e
f
g
h
i
j
k
l
m
n
footpad anti-virus
footpad anti-CrmD
Spleen H&E
Liver H&E

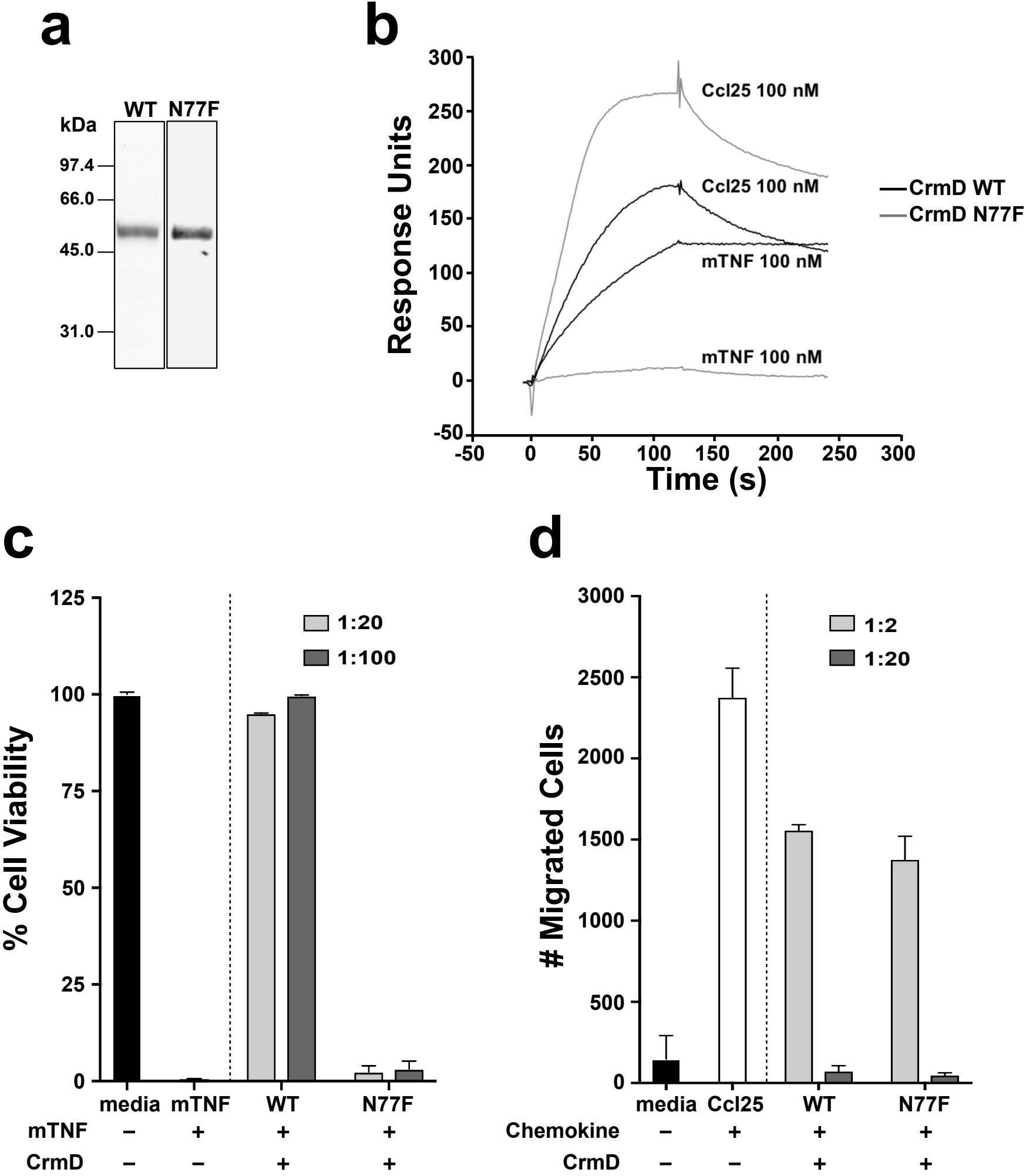
a
WT
N77F
kDa
97.4
66.0
45.0
31.0
b
Response Units
Time (s)
Ccl25 100 nM
Ccl25 100 nM
mTNF 100 nM
mTNF 100 nM
CrmD WT
CrmD N77F
c
% Cell Viability
1:20
1:100
media
mTNF
WT
N77F
mTNF
CrmD
d
Migrated Cells
1:2
1:20
media
Ccl25
WT
N77F
Chemokine
CrmD

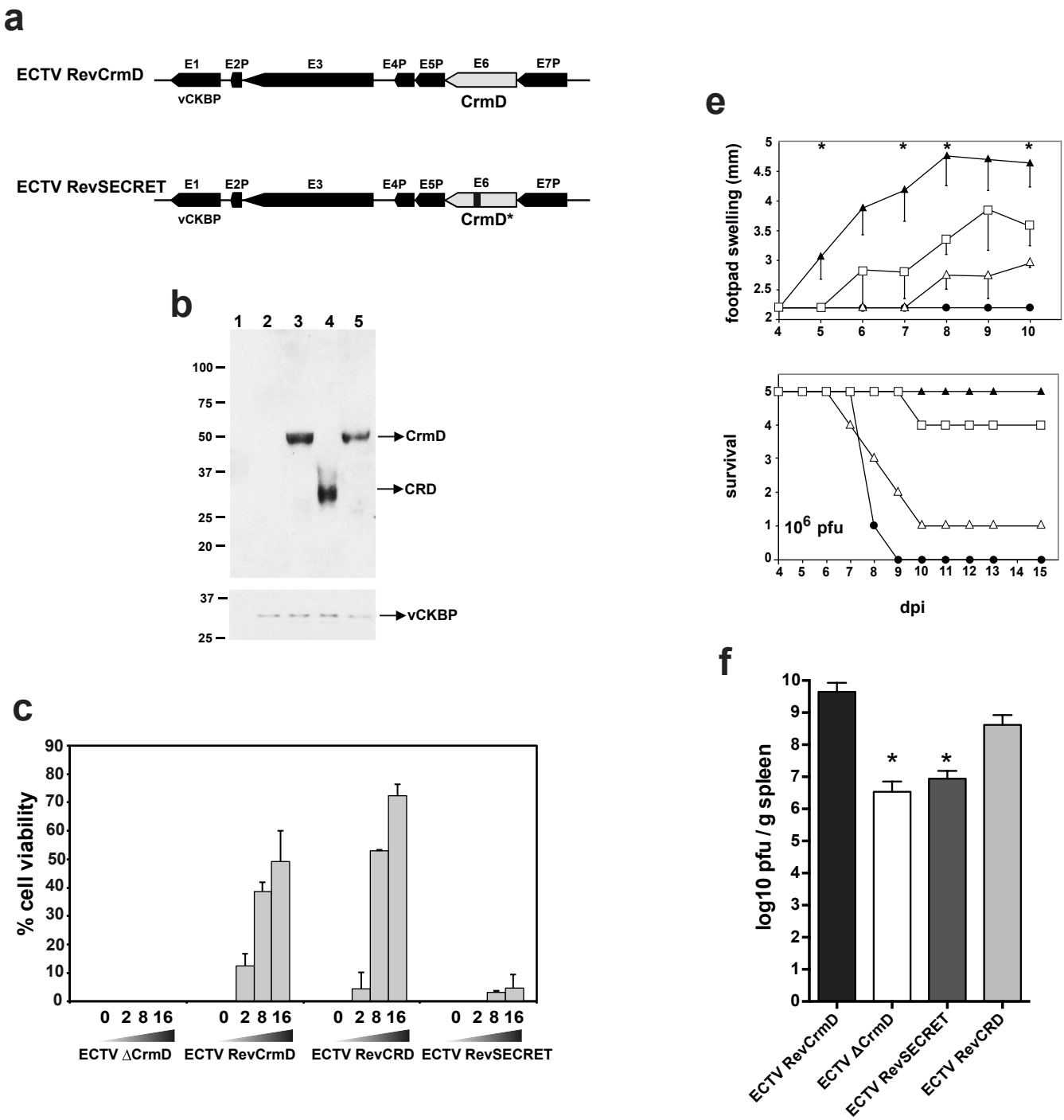

Dose (PFU)	ECTV RevCrmD survivors	ECTV RevCrmD MTD	ECTV ΔCrmD survivors	ECTV ΔCrmD MTD	ECTVRevCRD survivors	ECTVRevCRD MTD	ECTVRevSECRET survivors	ECTVRevSECRET MTD
10e4	0/5	8.2	5/5	n.a.	4/5	11.0	3/5	11.5
10e5	0/10	8.2	9/10	15.0	7/10	8.0	8/10	10.0
10e6	0/5	8.2	5/5	n.a.	1/5	8.5	4/5	10.0

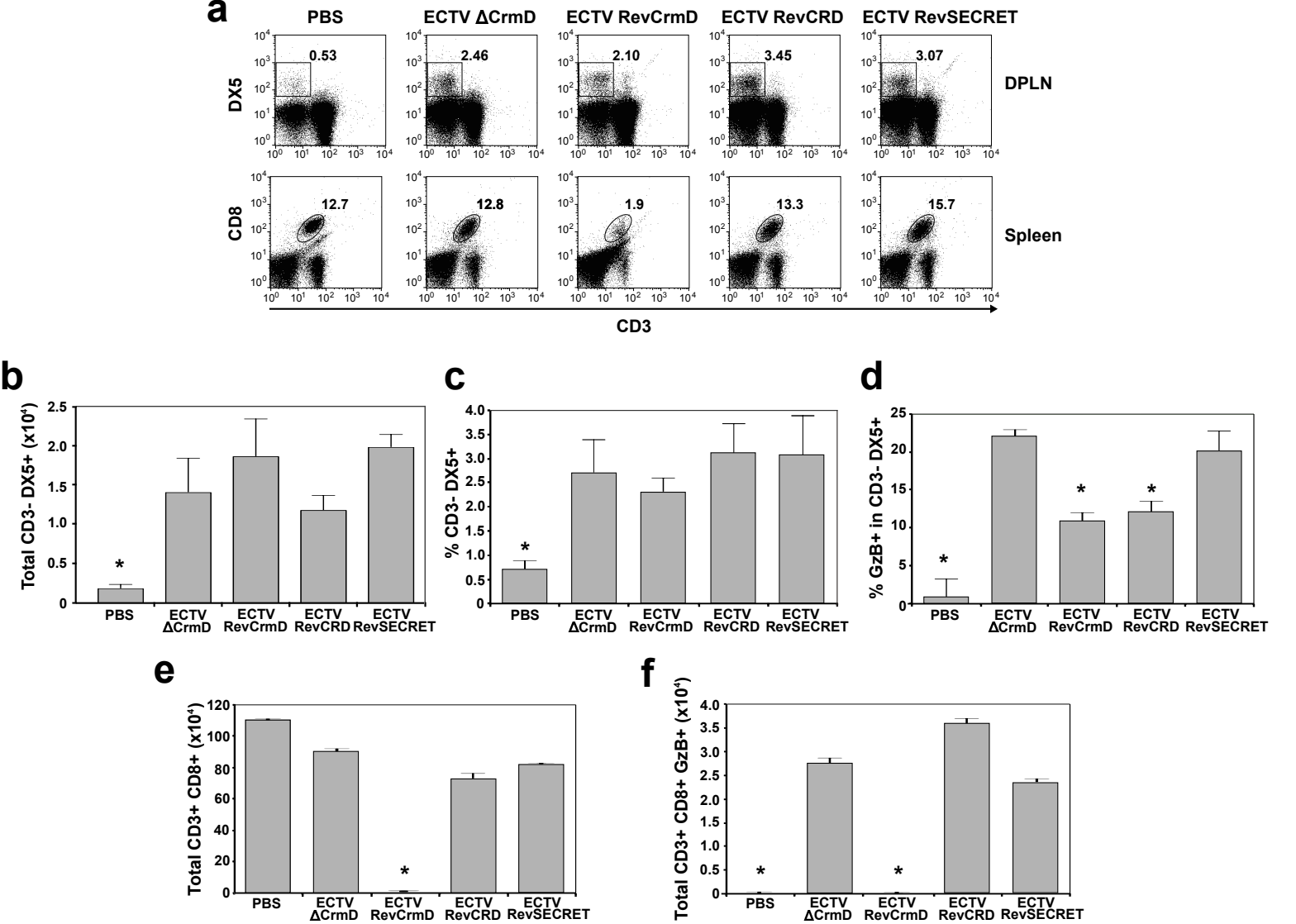
a
PBS
ECTV ΔCrmD
ECTV RevCrmD
ECTV RevCRD
ECTV RevSECRET
DX5
CD8
CD3
0.53
2.46
2.10
3.45
3.07
12.7
12.8
1.9
13.3
15.7
DPLN
Spleen
b
Total CD3- DX5+ (x10⁴)
c
% CD3- DX5+
d
% GzB+ in CD3- DX5+
e
Total CD3+ CD8+ (x10⁴)
f
Total CD3+ CD8+ GzB+ (x10⁴)
PBS
ECTV ΔCrmD
ECTV RevCrmD
ECTV RevCRD
ECTV RevSECRET

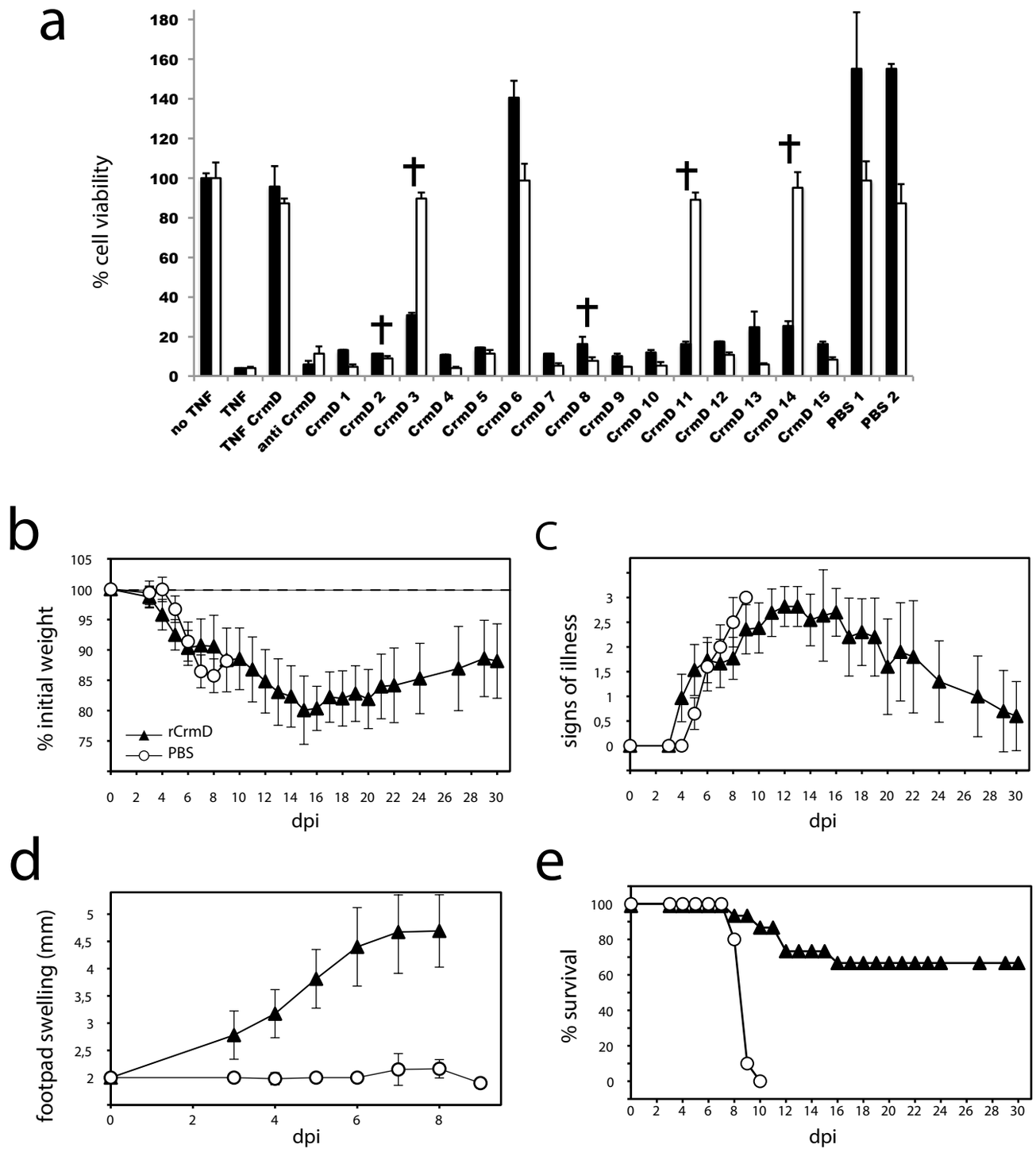
a
% cell viability
180
160
140
120
100
80
60
40
20
0
†
no TNF
TNF
TNF CrmD
anti CrmD
CrmD 1
CrmD 2
CrmD 3
CrmD 4
CrmD 5
CrmD 6
CrmD 7
CrmD 8
CrmD 9
CrmD 10
CrmD 11
CrmD 12
CrmD 13
CrmD 14
CrmD 15
PBS 1
PBS 2
b
% initial weight
105
100
95
90
85
80
75
rCrmD
PBS
0 2 4 6 8 10 12 14 16 18 20 22 24 26 28 30
dpi
c
signs of illness
3
2,5
2
1,5
1
0,5
0
0 2 4 6 8 10 12 14 16 18 20 22 24 26 28 30
dpi
d
footpad swelling (mm)
5
4,5
4
3,5
3
2,5
2
0 2 4 6 8
dpi
e
% survival
100
80
60
40
20
0
0 2 4 6 8 10 12 14 16 18 20 22 24 26 28 30
dpi